Evaluation of Crashworthy Battery Integration for a Medium-Lift Hybrid-Electric Helicopter using Full-Scale Simulation

E. Wegener¹, M. Waimer² and P. Schatrow.³

German Aerospace Center – Institute of Structures and Design, Stuttgart, Baden-Württemberg, 70569, Germany

Introducing battery technology as energy storage in aviation introduces challenges in crashworthiness. Balancing the integration of additional components, while minimizing their impact on post-crash hazards for occupants and individuals on ground is crucial to achieve a safety level equivalent to traditional propulsion architectures. This paper gives a brief overview of the requirements and methodologies for integrating batteries into a hybrid-electric propulsion architecture for medium-lift helicopters. Capitalizing on insights from conventional fuel tank crashworthiness technology, the aim is to effectively facilitate the adoption of battery technology in aviation applications. The paper focuses primarily on the evaluation of full-scale numerical crash simulations undergoing load cases ranging from certification to robustness. The shown simulated models feature a medium-lift helicopter with an example of an integrated battery energy storage. The evaluation includes the introduction of methodologies for battery surrogate models that can be used to evaluate thermal runaway originating from crash-induced mechanical deformation.

I. Nomenclature

CRBS = Crash-Resistant Battery System
CRFS = Crash-Resistant Fuel System
DLR = DLR German Aerospace Center

EASA = European Union Aviation Safety Agency

H/C = Helicopter

eVTOL = Electric Vertical Take-Off and Landing

FAA = Federal Aviation Administration

FE = Finite Element

MOC = Means of Compliance

MTOM = Maximum Take-Off Mass

NASA = National Aeronautics and Space Administration

SC-VTOL = Special Condition-VTOL (EASA) VTOL = Vertical Take-Off and Landing

II. Introduction

The transportation sector, including the aviation industry, is actively working on innovative solutions to decrease CO₂ emissions and support global climate objectives. One innovative approach to reduce emissions for medium-lift

¹ Scientific Researcher, Structural Integrity Department, Young Professional.

² Scientific Researcher, Structural Integrity Department, Professional.

³ Scientific Researcher, Structural Integrity Department, Professional.

helicopter (H/C) is the introduction of hybrid-electric drivetrains into the propulsion architecture. Naturally, hybrid-electric propulsion requires new energy storage systems compared to conventional fuel systems that are highly sophisticated in today's H/C technology.

In the past, the Federal Aviation Administration (FAA) launched the development of Crash-Resistant Fuel Systems (CRFS) in aviation applications by designing and introducing crash-resistant fuel tank features into the market, like self-sealing breakaway valves. The timeline of these efforts, dating back to the 1940s, is detailed in [2]. Throughout the following decades, research expanded to include the introduction of innovative bladder materials [3, 4], self-sealing breakaway valves [5], attachment mechanisms [5] and the realization of various drop tests [4–7]. Key contributors besides the FAA included the U.S. Army, U.S Air Force and the National Aeronautics and Space Administration (NASA). The development efforts resulted in the establishment of multiple criteria for the design and integration of CRFS, detailed in Chapter III-D.

Military applications played the primary role in advancing CRFS technologies in this time period. By 1994, it was concluded that no further scientific breakthroughs were required to implement CRFS in civil aviation [8]. The FAA responded by adding new amendments to airworthiness standards Part 27 and Part 29, integrating successful military rotorcraft strategies with reduced requirements to suit the less severe crash environments in civil aviation. Similar adjustments were made in the European Union Aviation Safety Agency's (EASA) airworthiness standards CS-27 and CS-29.

Adopting battery technology for energy storage introduces challenges in crashworthiness. Balancing the integration of additional components, while minimizing their impact on post-crash hazards for occupants and individuals on ground is crucial to achieving a safety level equivalent to traditional propulsion architectures with long safety history as for the above discussed CRFS.

This paper first covers the necessary requirements and methodologies for integrating batteries into the current propulsion architecture of medium-lift H/C. Afterwards, an exemplary energy storage design with integration in the crash zone is introduced and evaluated in full-scale simulations. Capitalizing on insights from conventional fuel tank technology, the aim is to effectively facilitate the adoption of battery technology in aviation operations.

III. Battery Crashworthiness Integration Methods

The design of an energy storage system is crucial for a H/C to achieve its design objectives and operate safely across the entire flight envelope. In addition, a crash-resistant energy storage system must adhere to specific criteria to prevent or minimize hazards in the event of a crash. Modern CRFS are required to withstand crash impacts and conditions considered severe but survivable for occupants, which may include significant structural damage. With the progress in crash survivability technologies, such as improved seats and restraints, systems enabling passengers to endure severe crashes that might otherwise destroy the aircraft have become crucial. Therefore, it is essential that the energy storage system is designed to meet these strict requirements.

A. Authority Regulations

To the authors knowledge, EASA currently lacks a standardized regulatory framework specifically dedicated to hybrid-electric propulsion systems for Vertical Take-Off and Landing (VTOL) applications. Consequently, all relevant EASA certification regulations have been thoroughly reviewed, including CS-27 [9], CS-29 [10], Special Condition E-19 for Electric / Hybrid Propulsion System [11], and Special Condition for VTOL (SC-VTOL) [12].

CS-29, the regulation for large and medium-lift rotorcraft serves as the foundation for the requirements discussed in this paper. Although SC-VTOL specifically targets electric VTOL (eVTOL) configurations rather than H/C, the authors anticipate that EASA will extend the application of SC-VTOL requirements to hybrid-electric H/C in the future. For the purpose of developing crash-safe battery integration concepts, the following key aspects can be extracted from SC-VTOL's requirements, which, in many instances, originate from CS-27 and CS-29:

1. Emergency Landing Conditions

Regulation CS-29.561(d) [10] mandate that the fuselage structure surrounding internal fuel tanks located beneath the passenger floor level must be engineered to withstand specific ultimate inertia load factors. This requirement ensures the structure is capable of preventing potential ruptures of the fuel tanks due to loads applied on this area.

In addition, SC-VTOL under MOC VTOL.2270(b)(1) [13] specifies that battery integration below the cabin floor may result in the underbody design being considered "non-traditional". In such instances, separate demonstration must be provided that the updated underbody structure features damping properties to limit acceleration to below 30 g in impact scenarios, as outlined in CS27.562(b)(1) [9]. Note, that the equivalent for large rotorcraft CS-29.562(b)(1) [10] depicts the same requirements. Consequently, considerable effort must be expected in the approval process.

2. Energy Storage Crash Resistance

As outlined in MOC VTOL.2325(a)(4) (Issue 2) [13], batteries installed as energy storage units are required to undergo a drop test with batteries charged to its most critical condition from a height of 15.2 m (50 ft). The primary objective of this test is to confirm the safety of the batteries post-crash, specifically ensuring that no leakage or fire ensues. However, if such incidents do occur, the test aims to demonstrate that they can be effectively controlled and contained for at least 15 min.

Therefore, crash-resistant battery integration concepts must guarantee robustness and safety under such testing conditions. This requirement is reflective of the standards described in CS-29.952 [10] concerning the crash resistance of fuel systems. It emphasizes a similar level of safety applied to traditional fuel systems and newer battery energy storage implementations.

3. Energy Retention Capability in an Emergency Landing

According to MOC VTOL.2430(a)(6) (Issue 2) [13] the drop test, as outlined in the previous paragraph, is also required to be conducted on water. It is crucial to demonstrate that the batteries' electrical energy poses no hazard post-impact with water, ensuring the safety of the occupants and any individuals in the water.

The presented research work focuses on "Limited Overwater Operations". Given this mission requirement, the specific drop test on water can be performed from a reduced height of only 6 m [14].

B. Battery Integration Concepts

Developments in electromobility are already well-advanced in the automotive industry, where crash safety is also a critical concern. Currently, the "Safety Cell" concept is widespread in the automotive industry. This concepts' typical integration zone on a H/C can be seen in Fig. 1. Its design principles aim to prevent battery penetration and deformation during a crash through the use of very stiff surrounding structures. However, this approach results in added weight, which is not ideal for the typically lightweight requirements of aviation applications.

Emerging developments are focusing on allowing deformation of the battery, thereby permitting "Mechanical Overload". The main advantages of this approach include:

- 1) Significant weight reduction due to less rigid structure
- 2) Smaller battery volume through denser cell packaging within the battery module
- 3) Increased flexibility in installation space, enabling battery integration even in crash-prone areas

In conclusion, two distinct concepts for battery integration can be identified. The first, termed the "Safety Cell" concept, is a conservatively safe approach that integrates the battery based on the safety cell principle, prohibiting any mechanical overloading. This concept oftentimes includes installing the battery outside the crash zone. The second approach, called the "Mechanical Overload" concept, is a more progressive yet still safe approach that permits mechanical overloading. Implementing this concept involves a thorough analysis of the battery and its integration into the surrounding structure. It further includes measures for safe containment of potential battery thermal runaways. Specific means of battery protection and containment for a "Mechanical Overload" design are documented in Chapter III-D.

C. Battery Integration Areas

Potential battery pack integration areas on a H/C are categorized in Fig. 1 based on the type of loads expected in the event of a crash that may lead to a thermal runaway of the battery. These loads include accelerations, localized penetrations and mechanical deformations.

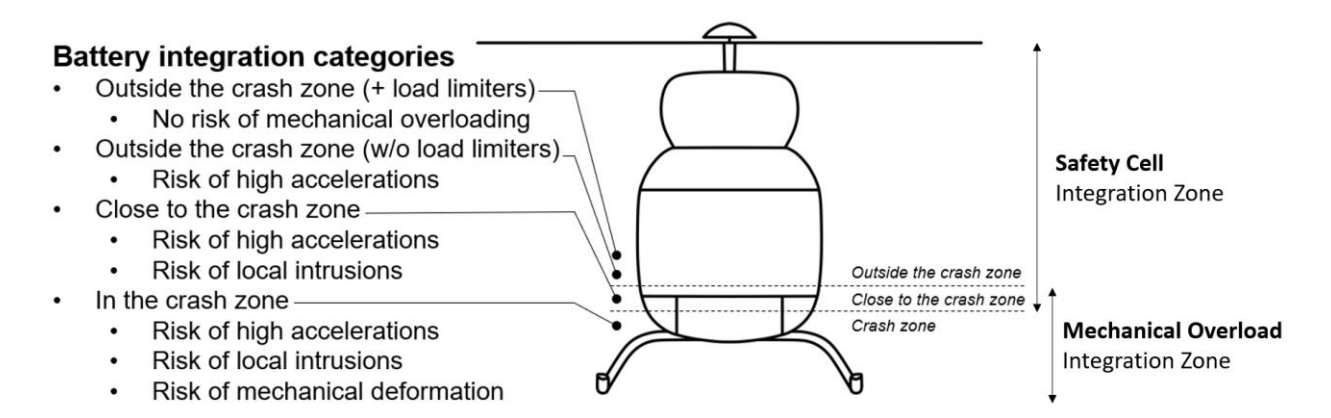


Fig. 1 Categories for crash-resistant battery integration in H/C.

A hybrid-electric drive system requires two distinct energy storage systems: a fuel tank and a battery. In the context of crash load scenarios, different integration combinations can be outlined and evaluated. Examples of these combinations are depicted in Fig. 2. Several criteria must be considered during the evaluation, including:

- 1) Regulatory aspects (e.g. CS-29.561(d) [10])
- 2) Expected design changes compared to traditional integration methods
- 3) Interaction with the surrounding structure
- 4) Crash energy absorption management
- 5) Robustness with regard to off-axis crash loads
- 6) Occupant evacuation
- 7) Firefighting
- 8) Interaction of fire load and ignition source

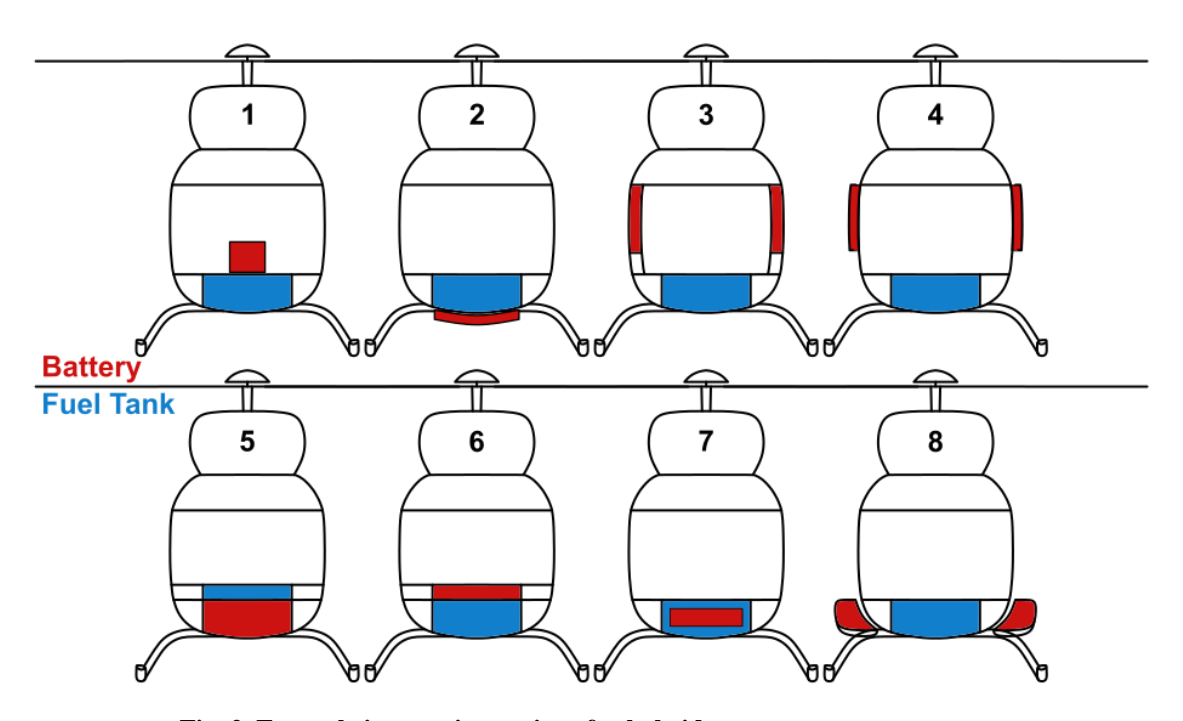


Fig. 2 Example integration options for hybrid energy storage systems.

One of the most promising approaches identified for the "Safety Cell" concept and visualized in Fig. 2 version 6 involves integrating the battery within a double floor. In this configuration, the battery is placed above the underbody structure, preserving a conventional subfloor design to ensure sufficient crash protection for the battery. Although this integration method is seen as safe and conservative, it may entail tradeoffs in cabin volume, particularly impacting cabin height, or necessitate a design with elevated airframe specifications.

A promising integration option within the "Mechanical Overload" safety concept can be seen in Fig. 2 version 8 and involves integrating the battery outside the airframe and alongside the underbody structure. In this setup, the battery is positioned in the primary crash zone while the underbody structure retains a traditional design.

Because of the advantages mentioned in the previous paragraph, the "Mechanical Overload" safety concept is investigated in more detail in this paper.

D. Crash-Resistant Battery System (CRBS) Guidelines

Based on traditional Crash-Resistant <u>Fuel</u> System (CRFS) methods and guidelines [15], generic guidelines for Crash-Resistant <u>Battery</u> Systems (CRBS) have been developed by the authors of this paper. They are meant to be used for crashworthy integration of crash-resistant battery systems into airframe structures.

These guidelines include a methodical approach of evaluating suitable integration zones based on the spatial position of the system relative to risk sources like the crash zone as well as occupants. These steps have already been described in the previous chapter.

The guidelines adopt a systems design approach, ensuring that each component is designed with consideration for the overall system's integrity, including crashworthiness. Recommendations on the mechanical design of the surrounding structure and attachment method are provided. Additionally, suggestions intended to reduce the risk to the distribution system (e.g. hoses, cables) and improve the impact and tear resistance of the overall system are included. Lastly, some guidance regarding controlling ignition sources is added. These methods have been published in a previous publication; refer to [16] for more detailed documentation.

IV. Model Development and Simplifications

A. Crashworthy Battery Integration Technology Bricks

Based on the preparatory work outlined in Chapter III, an exemplary battery storage design for a medium-lift H/C was created to demonstrate the developed integration methods. The integration design follows configuration 8 in Fig. 2, an external battery pod mounted alongside the H/C subfloor structure inside the crash zone. The integration concept follows the introduced "Mechanical Overload" approach, where the battery pack may experience severe mechanical loads under crash scenarios. To address the specific boundary conditions associated with this design, dedicated technology bricks were developed to mitigate challenges arising from these boundary condition. The developed exemplary battery storage is visualized in Fig. 3, featuring technology bricks identified and documented in a previous paper [16]. A short summary is given in this chapter.

To limit acceleration loads in the batteries in crash scenarios, load attenuation structures like crash absorbers are essential. In this application, volumetric absorbers, such as honeycomb structures, provide full-surface load introduction during crashes into the battery modules. These absorbers also significantly improve impact resistance as they typically compact with increased compression, doubling as protective shielding. Furthermore, these volumetric absorbers feature favorable crash behavior during crashes on uneven or soft impact surfaces or water impacts due to their spatial expansion.

Impact resistance is provided by the module housing. The casing material doubles as a containment layer during thermal runaway events. It can ensure safe conditions during thermal runaway events for a minimum of 15 min, up to temperatures of 1000°C. The containment layer is air- and watertight even under crash-induced stresses and deformations of the battery pod.

The venting system is realized with a single longitudinally running vent pipe positioned above the battery modules, safe during off-axis load cases and discharging thermal runaway products at the rear of the pod. The system ensures that emergency exits remain free of hot smoke and toxic gases. This effect is crucial in preventing excessive overpressure inside the battery and dissipates heat, reducing the risk and magnitude of thermal runaway propagation. The design aims to preserve the integrity of the battery system by allowing individual battery modules to detach from one another while the vent pipe is flexible enough, e.g. by accordion-like design, to follow individual module movements. This design removes the need for a secondary containment layer in case of large battery pack deformations, resulting in a positive impact on the overall weight of the system. Note that the pipes are only modelled as beam elements in the figure.

The primary structure of the pod was designed following traditional crashworthiness design principles, incorporating a stiff load-bearing "floor" structure providing structural integrity even under crash conditions and positioned between the battery modules above and absorbers below. This offers additional stroke for the batteries and its position mitigates the risk of heat-induced damage during thermal runaway cases with venting.

A FE model of the introduced battery pod design was derived for the simulation campaign in Chapter V. The pod's structure was designed with metallic material properties based on Aluminum 2024 data. All parts of the pod were

connected with tie contacts. Each pod features 156,357 nodes, 52,385 shells, 79,836 solids, an average shell element size of 12.5 mm and weights approx. 350 kg.

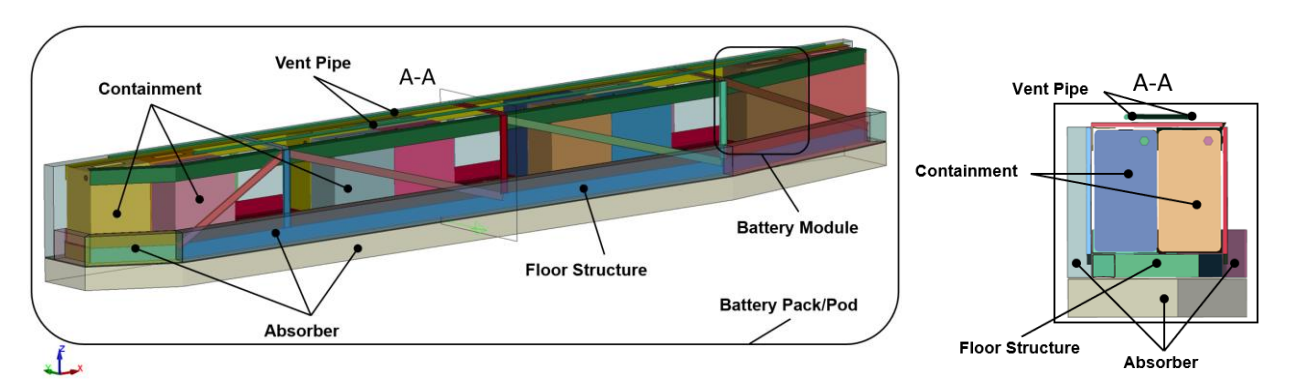


Fig. 3 Battery pod design concept.

No significant structural modifications to the H/C airframe are required, as the battery pod installation is not expected to compromise the survivable cabin volume of the occupants or be endangered by the kinematic behavior of the airframe during crash scenarios.

The structural connection between the pod and the H/C airframe is established through attachment points located at the front and rear main frames and the front landing gear bulkhead (see Fig. 4 (a)). The spacing in the module arrangement (battery pod packaging) prevents critical crash interaction between the modules and attachment points. This design only minimally affects the traditional airframe design and crash kinematics, where the underfloor structure of the H/C is utilized as a designated crush zone.

The attachment points have been engineered to fail under specific local loads, allowing for the separation of the battery pod and airframe structure (see Fig. 4 (b)). This feature is particularly important for robustness load cases, such as off-axis scenarios with roll angles, where the risk of interaction between the airframe and battery pod is increased. It additionally enables load attenuation at different acceleration levels for airframe (e.g. $a_z = 30$ g) and battery pod (e.g. $a_z = 200$ g).

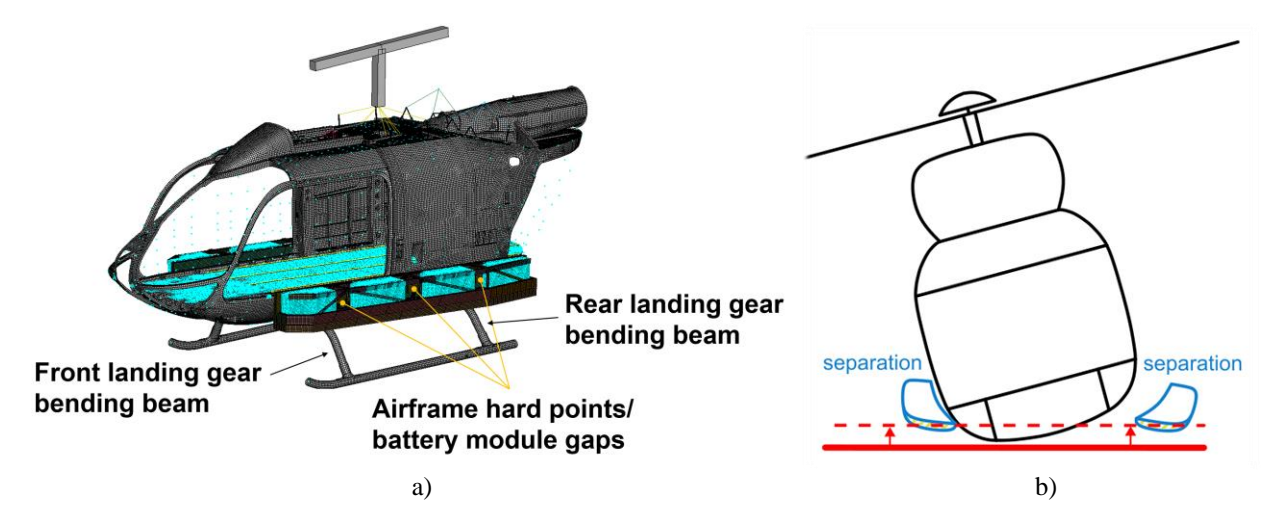


Fig. 4 Battery pod integration concept.

B. Generic Full-Scale Simulation Model

A generic full-scale Finite Element (FE) model of a medium-lift H/C incorporating the developed battery pod was created to assess the crashworthy battery integration concept. This comprehensive simulation was conducted to accurately capture the kinematic interaction between external battery pod, landing gear and H/C airframe. The model is visualized in Fig. 5.

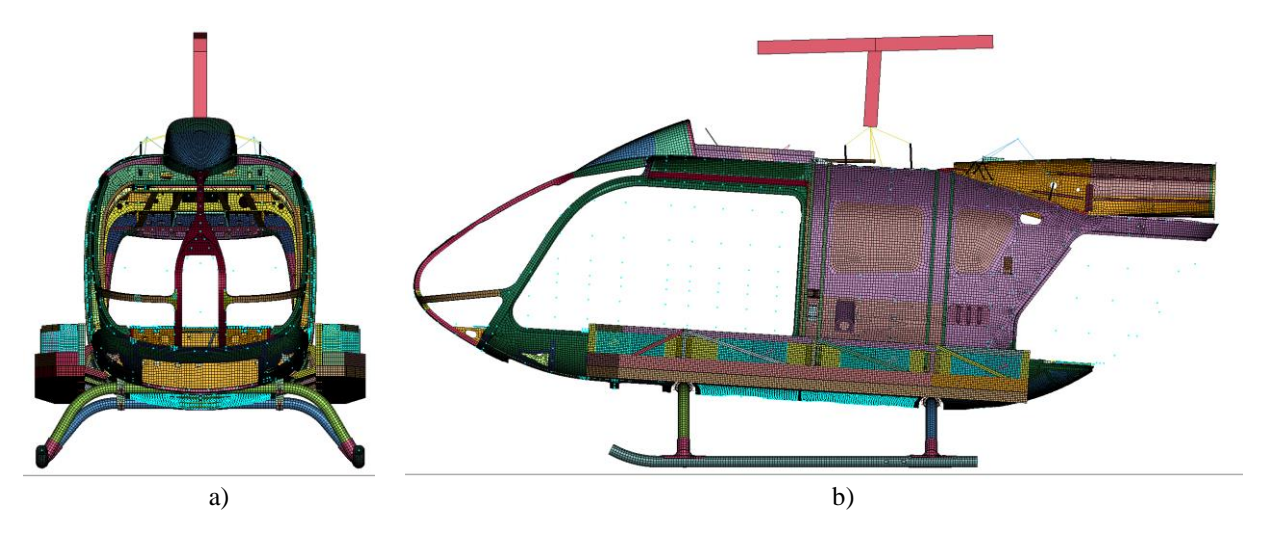


Fig. 5 Generic full-scale simulation model: (a) front and (b) side view.

Since this model is intended to assist in the evaluation of crashworthy battery integration, a partial validation of the model is conducted. Considering the critical role of the underfloor area in crash scenarios, the validation focused on the underbody structure of the H/C, including and particularly the landing gear. The pursued multi-step validation strategy can be seen in Fig. 6.

In a first step, inertia properties like mass, center of gravity and inertia tensors were compared to a generic medium-lift H/C design. In the second step of the validation, a reduced model, only featuring the landing gear, was compared to an available generic medium-lift H/C landing gear drop test. When comparing visually, displacement, vertical force, vertical acceleration and strain at specified locations, very good correlation between the test and simulation was established. In the third validation step, compliance to the CS-29.727 Reserve Energy Absorption Drop Test [10] was shown with very conservative assumptions. Kinematic effects from a historical full-scale crash test from a height of about 15 m were verified in a forth validation step of the airframe model [1]. It was concluded that the model features sufficient accuracy for load cases investigating crashworthy battery integration.

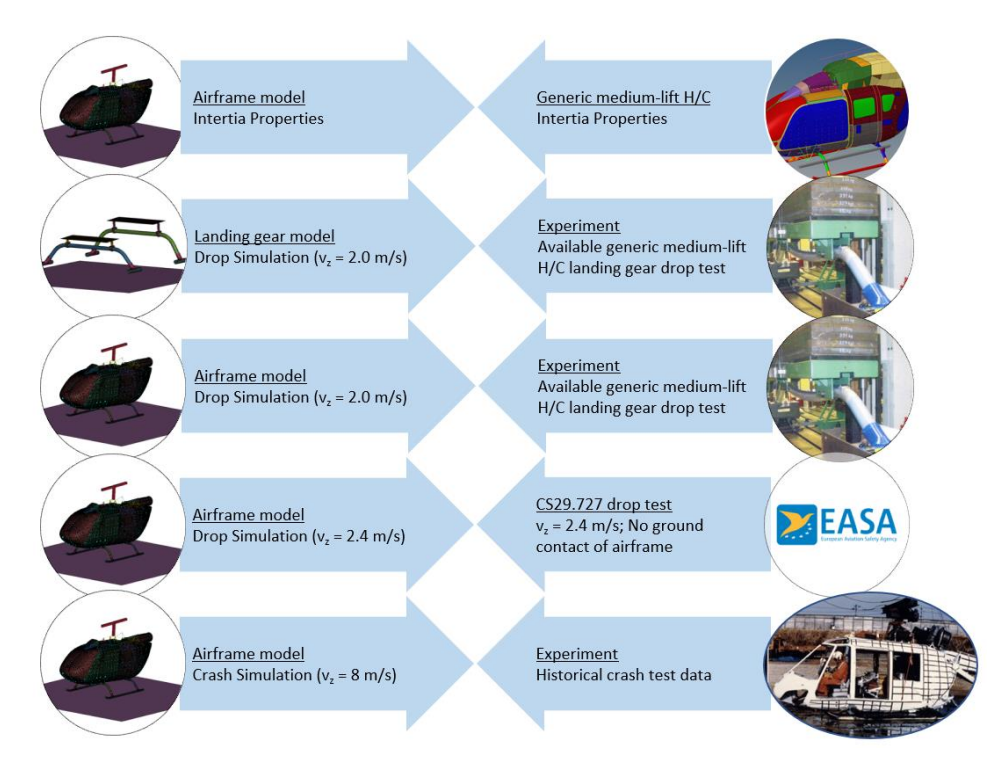


Fig. 6 Model validation strategy.

C. Surrogate Battery Models

Throughout different development phases, analysis methodologies of varying degrees of detail and efficiency are required. In early design stages, such as the conceptual design discussed in this paper, fast but adequately accurate techniques are required to model battery systems in tests and numerical simulations. In later, more detailed design stages when precision and accuracy become more significant, more detailed and complex models are required. A visualization of possible surrogate battery models for full-scale applications in a building block are shown in Fig. 7. The model fidelity level increases from the bottom to the top, first only depicting battery properties such as mass, followed by properties such as inertia, stiffness and more complex battery characteristics such as thermal and electrochemical effects.

All simulations of this conceptual design study feature battery surrogate models corresponding to the "Stiffness Level", featuring only a battery casing that models the mass, inertia and stiffness of a generic battery module. The batteries are examined at the module level, which achieves a balance between assessing the effects of entire battery packs and investigating individual battery cells. The internal battery module structure is not captured, mainly due to the lack of battery data at this early design stage, and hence structural deformation of the surrogate model is not validated. These limitations in battery surrogate modelling and in the definition of proper thermal runaway criteria is subject of current research work at DLR.

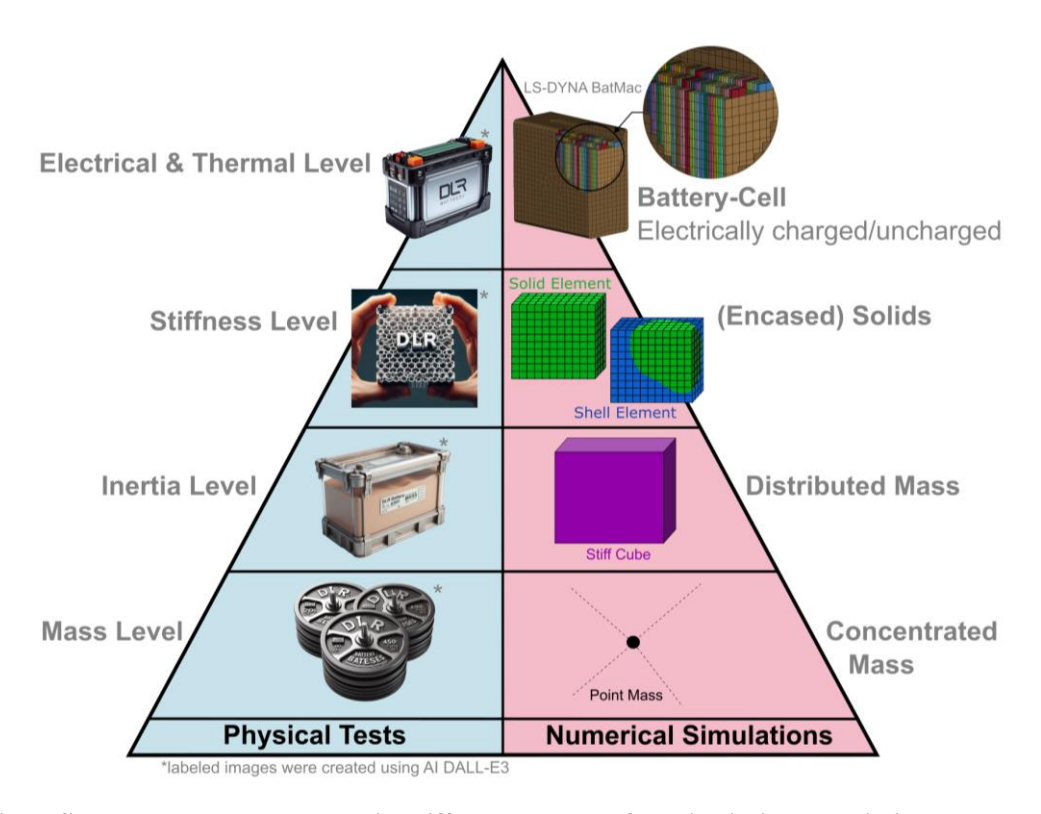


Fig. 7 Surrogate battery models with different degrees of detail within the Building Block.

Using battery surrogate models, quantitative pass/fail criteria must be established to evaluate the risk of thermal runaway. Since the battery surrogate models used in this paper's studies only modelled inertia, mass and stiffness of a potential battery module, the 'acceleration' and 'internal energy' metrics were evaluated. In this paper's evaluation, a quantitative pass/fail criterion of accelerations surpassing 200 g was assumed based on literature and experience values.

Preliminary studies have shown, that an increase in structural complexity of the integration structure typically also increases acceleration oscillation and is strongly depended on the selected local point of measurement. This effect was observed when simulating single battery modules or the entire battery pod. The design goal of a crush plateau at accelerations of 200 g was shown at some battery modules. At other modules however, presumably the increase in structural complexity and impact velocity also increased acceleration oscillation. This also increased the difficulty of evaluating the risk of a thermal runaway during crash based on measured accelerations.

All acceleration results were filtered with SAE J211-1 [17] CFC60 filter. This increased the readability of the acceleration results, but not enough to compensate for the described effects.

This leads to the consideration of whether 'acceleration versus pulse duration' may be a more suitable criterion for thermal runaway evaluation at airframe integration level. However, such an evaluation criterion requires more detailed battery test data.

Therefore, the internal energy of each battery module was additionally evaluated as an alternative measure for the assessment of thermal runaway. This method enables the observer to study the effect of crash conditions on selected battery modules based on their change in internal energy – as a measure of structural loading respectively structural deformation. While residual internal energy represents material damage, failure, and plastic deformation, elastic deformation can also be analyzed based on short term internal energy changes. This method is particularly useful in evaluating the risk of thermal runaway across multiple battery modules, identifying the biggest source of thermal runaway risk for more detailed evaluations. However, an absolute risk assessment based on this criterion requires battery test data and differentiation of load types like local indentation and global deformation of the battery model. Following this approach, potential modelling simplifications of the battery modules must be considered, as they may affect the measure of internal energy and consequently the assessment of crash impacts.

V. Full-Scale Simulation

A. Simulation Matrix

To study the integration of the batteries into the structural environment, several preliminary case studies were conducted. The battery modules were first simulated as single models, then integrated into the battery pod and finally the simulations considered the battery pod mounted on a generic medium-lift full-scale H/C airframe. This multi-step approach ensured that the absorber design, the battery packaging, the pod structure and the attachment between pod and airframe feature the desired crashworthy performance.

The full-scale FE model with integrated battery pods features 521,084 nodes, 3,193 beams, 313,471 shells, 160,112 solids and an average shell element size of 12.5 mm. All mentioned simulations were simulated using the commercial FE code LS-DYNA, version 13.1.0, with boundary conditions described in this paragraph. All simulations were executed on 4 nodes simultaneously on a workstation with each node featuring the following properties: processor: 2x 16-cores AMD EPYC "MILAN" 7313, memory (RAM): 16x 64 GB (DDR4 3200 MHz), hard disk drive: 500 GB Crucial P5 Plus SSD. The average simulation time was approx. 21 hours.

Relevant crash regulation for the application presented in this paper are summarized in Chapter III-A. Based on these requirements, a simulation matrix was established, see Table 1, specifically suited for the evaluation of the presented battery integration design described in Chapter IV.

After integrating the battery pod at the airframe, boundary conditions from CS-29.727 Reserve Energy Absorption Drop Test [10], where any part of the H/C but the landing gear may not touch the ground, were used to confirm compliance with present regulation.

The impact velocity was then increased to values mandated in CS-29.562 Emergency Landing Dynamic Conditions [10]. In this reference load case for "emergency landing" conditions, as defined in MOC VTOL.2270 [13], variations investigating the effect of horizontal velocity and airframe orientation on the crash kinematics were simulated.

Representative boundary conditions of the "survivable emergency landing" are derived from MOC VTOL.2325(a)(4) (Issue 2) [13]. To ensure robustness, variations with off-axis orientations and additional horizontal velocity are investigated. Please note that this "survivable emergency landing" condition is not applied for the assessment of occupant injuries, survivable volume, mass retention and maintenance of evacuation paths. Solely the prevention of post-crash hazards, mainly post-crash fire of the battery pod, is evaluated.

Finally, the battery integration was simulated against further robustness load cases to evaluate their influence on the configuration's behavior. This includes changes to the impact surface like sloped terrain, which would result in more localized crash loads on the battery system, soft soils and impact on water and their effect on crash kinematics.

Note that all interactions with the impact surface featured a friction coefficient of μ =0.19.

Table 1 Simulation Matrix.

Reference load case	vz [m/s]	v _x [m/s]	roll, pitch, yaw [°]	Terrain
CS-29.727:	2.4	0.0	0, 0, 0	Rigid, flat
Reserve Energy Absorption				
Drop Test				
Based on CS-29.562:	7.9	0.0-4.57	0-30, 0-10, 0-10	Rigid, flat
Emergency Landing Dynamic				
Conditions (injury assessment)				
CS-29.952:	17.3	0.0-4.57	0-30, 0-10, 0-10	Rigid, flat
Fuel System Crash Resistance				_
Robustness	17.3	0.0	0, 0, 0	Rigid, flat, sloped, blunt
				obstacles, soft soil, water

B. Full-Scale Simulation Study

In this paper, the baseline load cases of CS-29.727: Reserve Energy Absorption Drop Test [10], CS-29.562: Emergency Landing Dynamic Conditions [10] and CS-29.952: Fuel System Crash Resistance Test [10] without off-axis boundary conditions and horizontal velocity are documented in detail as they have proven to be effective in providing insight into the behavior of the designed battery pod with surrounding structures during crash.

1. CS-29. 727: Reserve Energy Absorption Drop Test

The airframe in this load case impacts the ground with a vertical velocity of 2.4 m/s with flat skids. The load case is derived from CS-29.727: Reserve Energy Absorption Drop Test [10]. This regulation describes the requirement that any part of the H/C but the landing gear may not touch the ground. In Fig. 8 (a)-(c) the maximum deflection of the landing gear can be seen, which occurs at 220 ms. Note, that an application of full lift (lift equal to maximum take-off mass (MTOM)) to the model is allowed but not applied in this simulation. Hence, the results show sufficient conservatism and compliance with the given requirement.

Very small interaction between the landing gear bending beams and the battery absorber at the pod underside can be identified. The interaction can be seen as imprints at the front and rear attachment points, here visualized as effective plastic strain at the port battery pod bottom absorber elements in Fig. 8 (d) and (e).

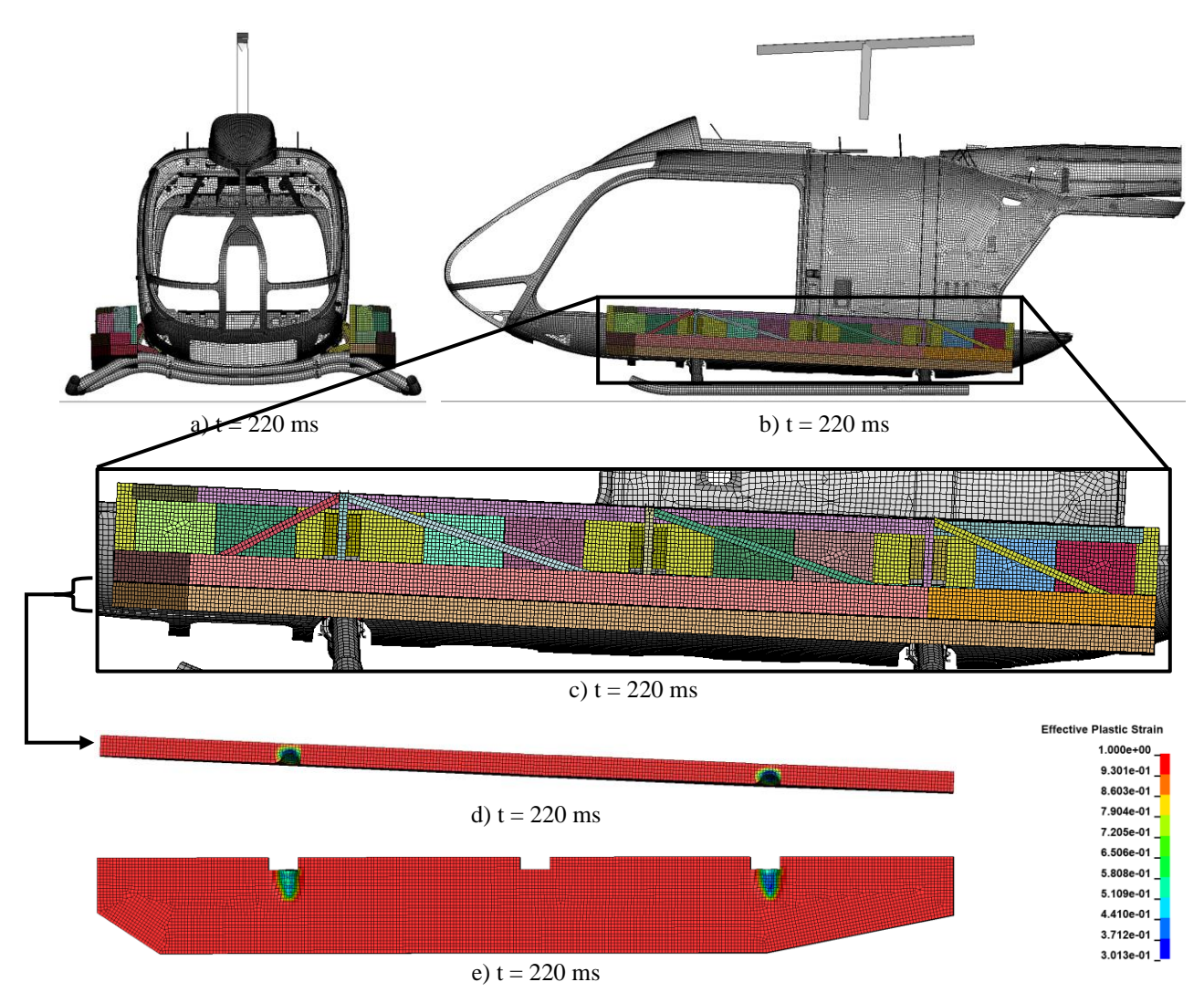


Fig. 8 Vertical impact with $v_z = 2.4$ m/s: Landing gear maximum deflection: (a) front, (b) side, (c) detail battery pod view and starboard bottom absorber effective plastic strain (d) inside and (e) bottom view.

One of the key components to ensuring energy conversion and stability in LS-DYNA crash simulations is checking the equation in Formula 1 that holds true at all times during the simulation.

$$E_{total} = E_{kin}^{t_0} + E_{int}^{t_0} + W_{ext} = E_{kin} + E_{int} + E_{si} + E_{hg}$$
 (1)

 $E_{kin}^{t_0}$ is the initial kinetic energy, $E_{int}^{t_0}$ the initial internal energy, E_{kin} the current kinetic energy, E_{int} the current internal energy, E_{si} the current sliding interface energy (including friction), E_{hg} the current hourglass energy and W_{ext} the external work.

These energy plots can be seen in Fig. 9. Almost all kinetic energy is absorbed by the landing gear and converted into internal energy as deformation. The increase in total energy originates from the increase in external work. External work includes work done by applied (external) forces, here the vertical displacement in the gravity field. After the maximum landing gear deformation is reached at 220 ms, the structure slightly rebounds.

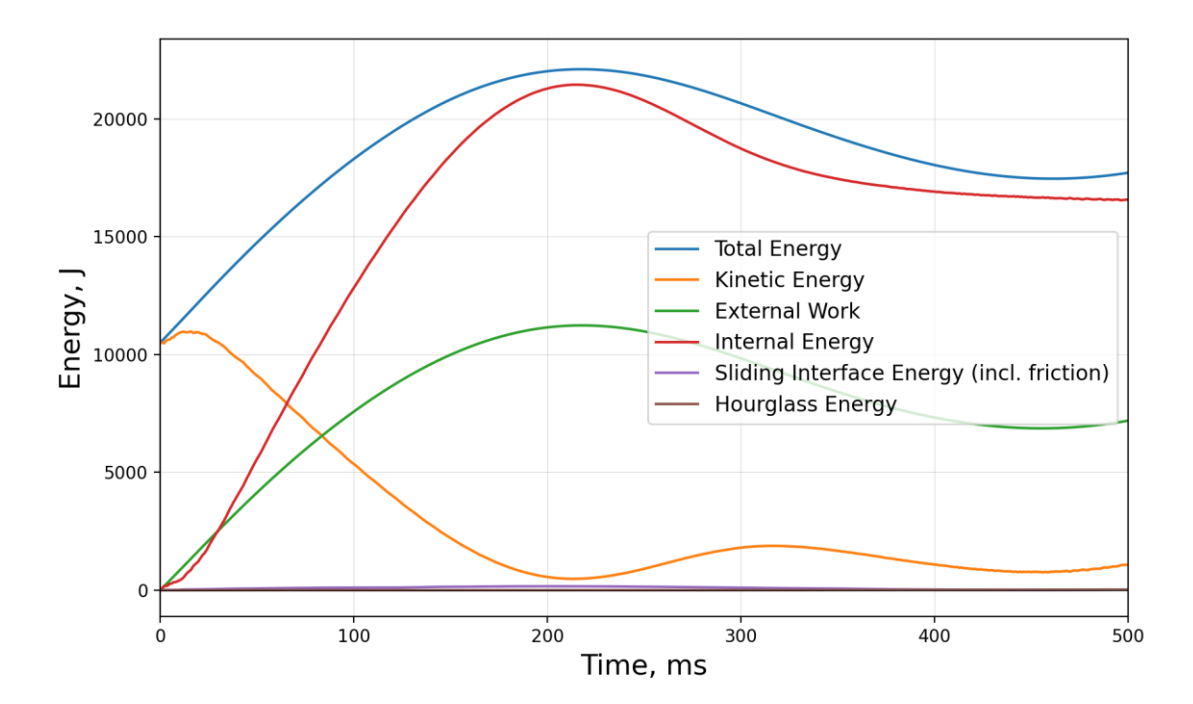


Fig. 9 Vertical impact with $v_z = 2.4$ m/s: Global energies.

As a result of this load case, the battery modules feature very small accelerations that stayed well within the defined limits of 200 g, and the battery pod structure and absorbers only feature negligible deformation.

Concluding, a successful demonstration of the CS-29.562 Reserve Energy Absorption Drop Test [10] with attached external battery pods is shown. With the additional batteries as external side pods attached to the airframe, no part but the landing gear is touching the ground. The main deformation is observed in the landing gear. Small contact interaction between the battery pod and landing gear is shown, which should easily be avoidable in a more detailed design stage. This interaction with the landing gear is considered small enough to show that the structural integrity and functionality of the landing gear is not compromised.

2. CS-29.562: Emergency Landing Dynamic Conditions

In this load case, the landing gear touches the impact surface at a vertical impact velocity of 7.9 m/s, which is derived from boundary conditions of CS-29.562 Emergency Landing Dynamic Conditions [10], referencing "emergency landing" conditions as defined in MOC VTOL.2270 [13]. Only the vertical aspect of this regulation load case is simulated. The combination with a horizontal impact velocity is part of the simulation matrix, but not discussed in this paper.

As can be seen in Fig. 10, the rear bending beam center of the landing gear impacts the ground at 50 ms (a), while the front one impacts the ground at 70 ms (b). This time shift is due to the angle of attack of the H/C airframe and correspondingly different bending beam heights compared to the landing gear skids (also see Fig. 5). Maximum deformation of the landing gear is reached at 130 ms (Fig. 10 (c)).

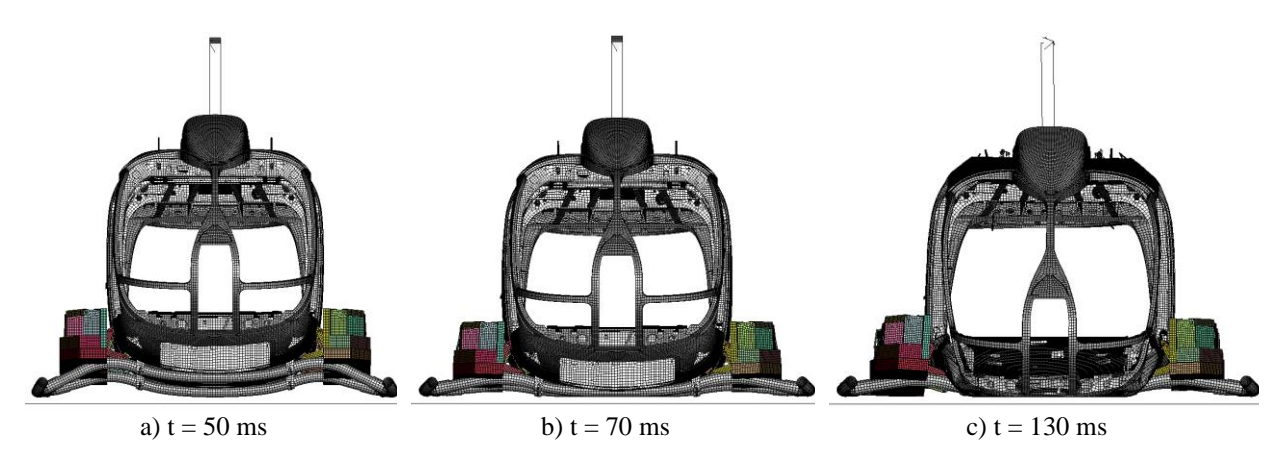


Fig. 10 Vertical impact with $v_z = 7.9$ m/s: (a) Rear and (b) front landing gear bending beam impacting the ground, (c) maximum deformation.

The battery pod response during maximum landing gear deformation at 130 ms is visualized in Fig. 11 in more detail. It can be seen in (b) and (c) that the battery pod installed at the airframe develops a hinge in its center position. During the crash event, the battery pod rests on the front and rear landing gear bending beams above the ground introducing bending loads in the battery pods that results in this hinge development. This hinge failure pattern is initiated at 35 ms with compressive buckling of the top structures of the battery pod.

The interaction between the battery pod and the landing gear is visualized as effective plastic strain of the pod bottom absorber in (f) and (g). The deformation of the absorber, which is fully stroked locally at interaction points with the landing gear, only minimally stroked outside of these landing gear interaction zones. Note that the tubular landing gear bending beams did not collapse under the battery pod crush load and maintained its circular cross-section which resulted in this local crushing of the battery pod absorbers.

The kinematics of the battery pod structure is significantly influenced by this interaction with the landing gear. The developed hinge in the center of the pod can be seen in (d) and (e) at the moment of maximum deformation. As the battery packaging considered large gaps at structurally hard points of pod attachment and airframe structure, this hinge development does not result in mechanical loading of the battery modules. The pod kinematics shows that more dense battery packaging might be critical as battery modules would crush into each other.

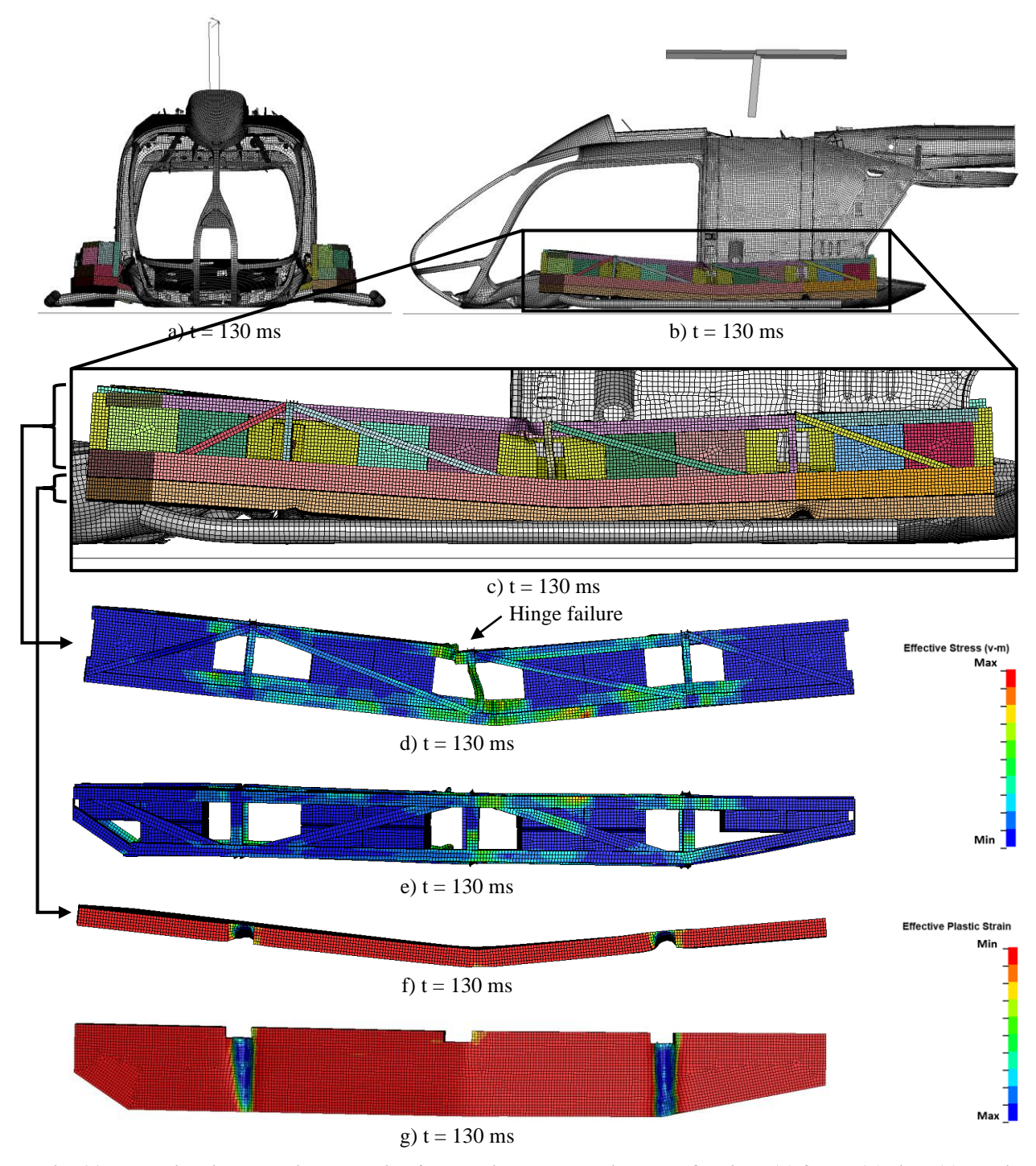


Fig. 11 Vertical impact with v_z = 7.9 m/s: Landing gear maximum deflection: (a) front, (b) side, (c) detail view, starboard structure von mises stress (d) inside and (e) bottom view and starboard bottom absorber effective plastic strain (f) inside and (g) bottom view.

The global energies of this load case can be seen in Fig. 12. The main crash phase occurs until approx. 130 ms, with subsequently only minor changes in kinetic and internal energy. The graphs show expected behavior with overall higher total energy levels compared to the load case in the previous paragraph because of the higher initial kinetic energy. This kinetic energy is almost completely converted into internal energy during the crash phase. External work is significantly higher compared to the load case in the previous paragraph, as the model undergoes more vertical

displacement in the gravity field due to more distinct deformation of the landing gear and underfloor structure. Some sliding interface energy can be observed, mainly due to the higher interaction of the airframe with the impact surface.

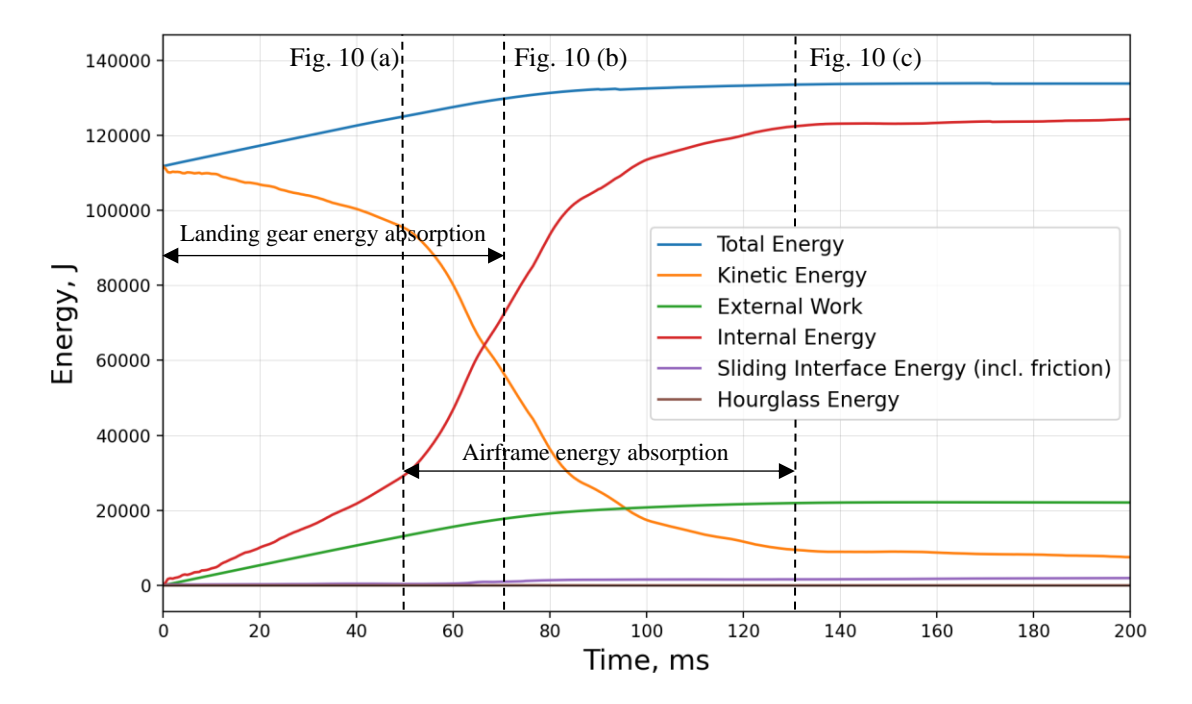


Fig. 12 Vertical impact with $v_z = 7.9$ m/s: Global energies.

For this representative emergency landing load case, the battery absorbers only marginally contribute to the overall energy absorption although their presence ensures protection for the battery modules. This is a reasonable result as the attachment concept ensures a certain degree of independent crash kinematics of the airframe and battery pod.

Battery module accelerations seen in Fig. 13 show high-frequency oscillations with peak values that partly significantly exceed the specified limit of 200 g. This is the case especially for modules installed inside or between the attachment locations, while the modules installed outside or forward of the front attachment and respectively behind the rear attachments stayed with the 200 g acceleration limit.

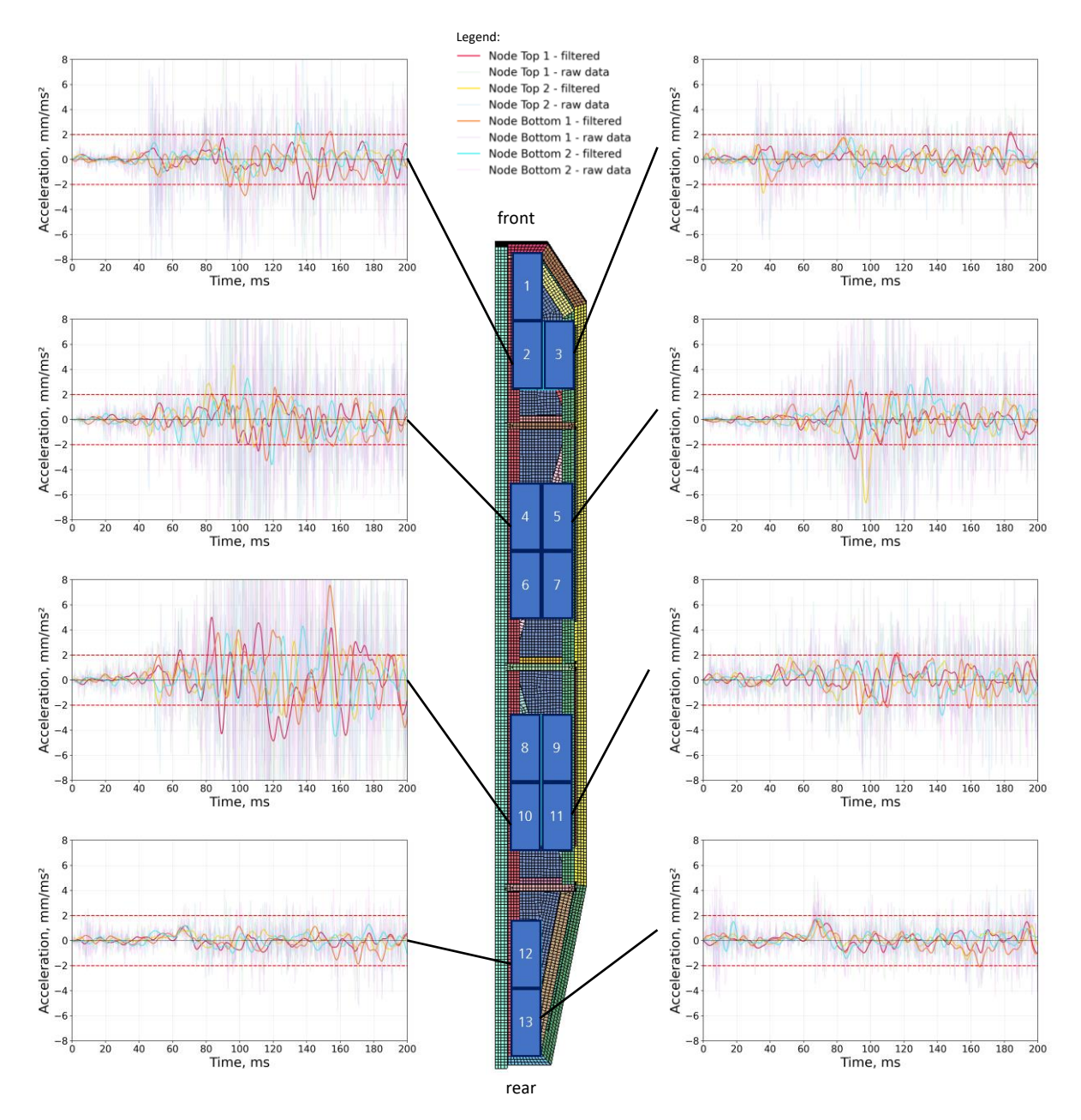


Fig. 13 Vertical impact with $v_z = 7.9$ m/s: Starboard module acceleration (filter: CFC60 $f_s = 2.0$ kHz).

As already mentioned in Chapter IV-C, the internal energies of the surrogate battery modules are also evaluated, and are shown in Fig. 14. First peaks in internal energy can be seen at approx. 65 ms for modules 10 and 12, which both are located at the inside of the pod and close to the rear landing gear. At the same time, module 11 located outside shows a significantly smaller peak. All three modules are close to the contact interaction of landing gear bending beam and battery pod, with more distinct crushing at the inner side which is reflected in the above discussed peaks of modules' internal energies. At approx. 85 ms peaks in internal energy for modules 2 and 4 can be seen, which are located at the forward landing gear bending beam. Again, lower peaks of outer modules 3 and 5 can be seen. At 85 ms, the battery pod impacts on the forward landing gear bending beam. This evaluation of internal energies indicates an increase in thermal runaway risk at inside and rear positions.

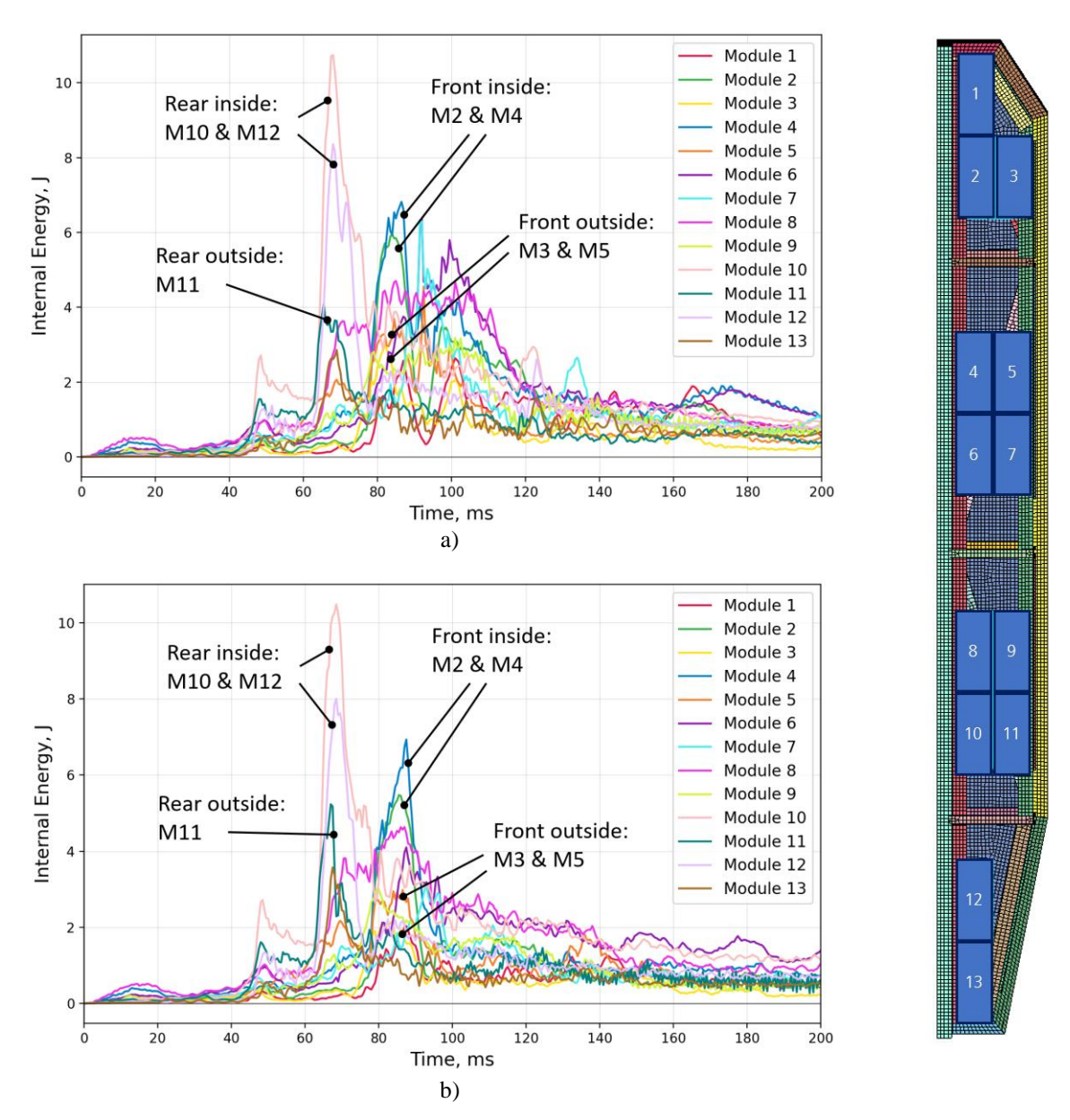


Fig. 14 Vertical impact with $v_z = 7.9$ m/s: Internal energy battery modules (a) port and (b) starboard.

The evaluation of acceleration and internal energy data shows slightly different trends. This discrepancy may originate from differences in model sensitivity or methodical assumptions regarding the quantitative pass/fail criteria. Determining which evaluation criterion provides more accurate thermal runaway representation is still an active area of research. However, internal energy evaluation may offer a broader perspective on the system's behavior, which potentially makes it a more suitable approach in full-scale analysis.

Summarized, this reference load case for the emergency landing category shows generally favorable crash kinematics. The battery acceleration peak loads partly exceed the acceleration limits which needs to be further evaluated in consideration of the peak durations, due to the high-frequency oscillations. As a major effect, the battery pod experiences a bending hinge development due to its contact interaction with the landing gear. This hinge deformation affects the battery pod installation volume. In case of a more densely pod packaging, the potential formation of a bending hinge and a corresponding intrusion of pod structures in this area needs to be considered.

3. CS-29.952: Fuel System Crash Resistance Test

In this load case, the impact velocity is derived from MOC VTOL.2325(a)(4) (Issue 2) [12] and represents the "survivable emergency landing" condition. This load case is originally aimed at energy storage integration studies,

where the energy storage and its surrounding structure is drop tested from a height of 15.2 m or 50 ft, as mentioned in Chapter III-A-2. This drop height leads to an impact velocity of 17.3 m/s.

Please note that this "survivable emergency landing" condition is not applied for the assessment of occupant injuries, survivable volume, mass retention and maintenance of evacuation paths. Solely the prevention of post-crash hazards, mainly post-crash fire, is evaluated. Hence, cabin collapse and severe airframe structural deformation can occur while the only evaluation criteria are the risks of post-crash hazards coming from the energy storage.

As seen in Fig. 15, the rear landing gear bending beam impacts the ground at 25 ms (a) and the front one at 30 ms (b). Maximum deformation of the H/C airframe is reached at 70 ms (c).

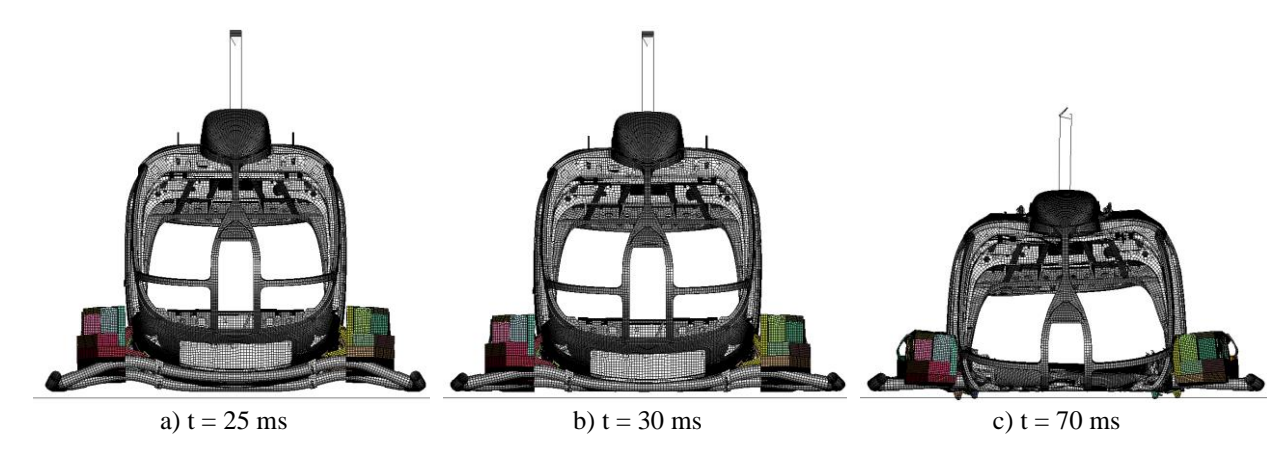


Fig. 15 Vertical impact with $v_z = 17.3$ m/s: (a) Rear, (b) front landing gear bending beam impacting the ground, (c) maximum deformation.

A detail view of the battery pod response after maximum deformation is reached at 70 ms is shown in Fig. 16. The battery pod bottom absorber is designed for this 50 ft drop test condition, its effective plastic strain is plotted in (f) and (g). The bending beam indentations can clearly be seen. Again, the bending beam tubes do not collapse and maintained its circular cross-section which deeply crush into the battery honeycomb absorber.

As a result, the local crash loads increase in those locations and lead to distinct local deformations of the above battery pod structure as can be seen in (d). This local deformation of the battery pod structure enables the entire bottom absorber surface to get in contact with the ground for further full-surface crushing and corresponding load attenuation.

In contrast to the previous load case with $v_z = 7.9$ m/s, a bending hinge does not evolve in this load case which is mainly attributed to the local deformation of the battery pod structure that enables the entire battery bottom absorber to get in contact with the ground. However, the upper longeron structures of the battery pod clearly shows stability failure in the center position which indicates that the development of a bending hinge was initiated.

This underlines the important design criterion that battery pod supporting structures need to consider crash aspects and must be designed in a way to prevent battery module intrusions – a key design parameter known from crash-resistant fuel tank system guidelines [16].

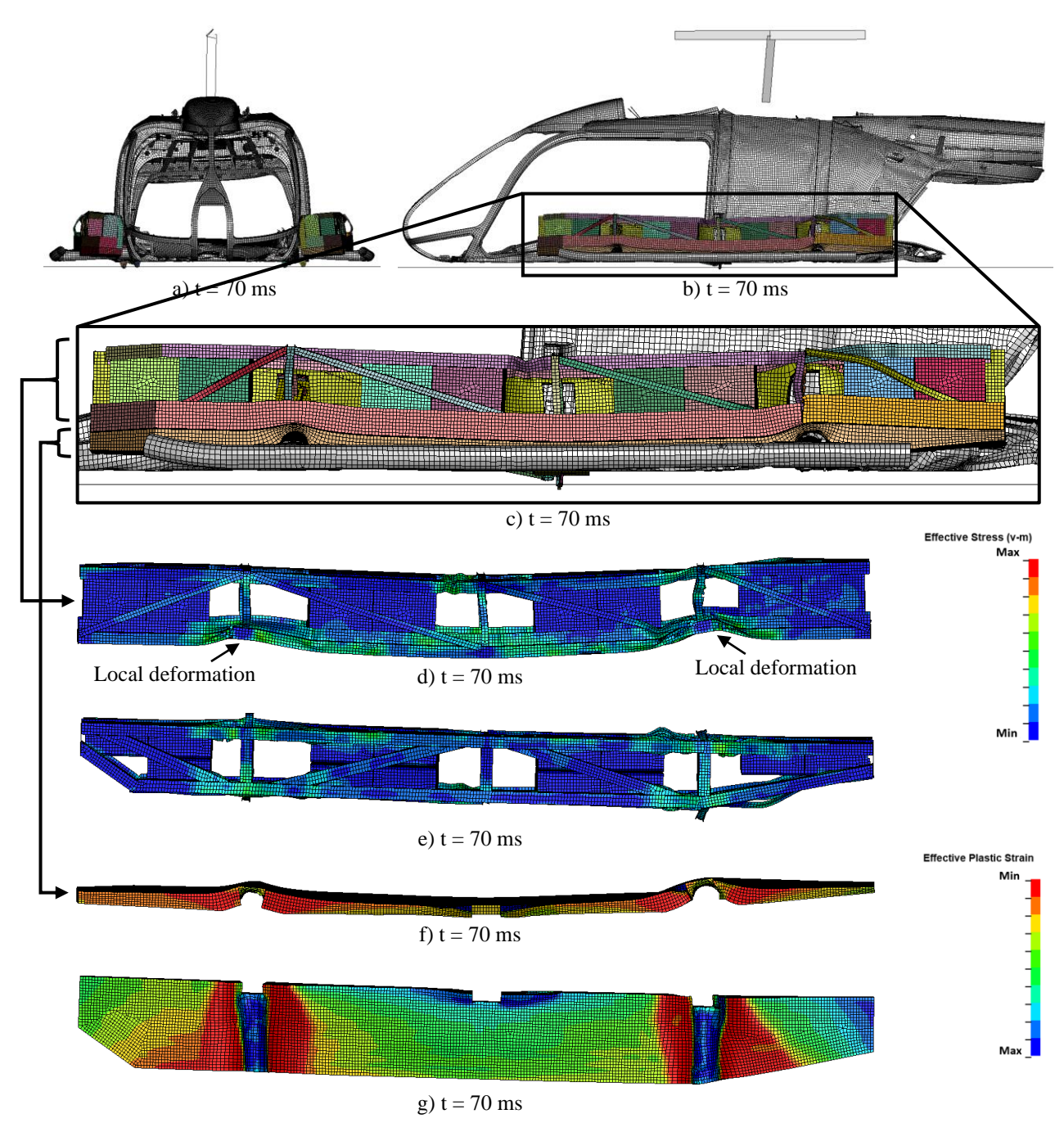


Fig. 16 Vertical impact with v_z = 17.3 m/s: Landing gear maximum deflection: (a) front, (b) side, (c) detail view, starboard structure von mises stress (d) inside and (e) bottom view. and starboard bottom absorber effective plastic strain (f) inside and (g) bottom view.

The global energy plot in Fig. 17 shows the expected behavior. The plot of curves is characterized by higher energy levels and steeper slopes compared to the "emergency landing" load case discussed before. The main crash phase ends at approx. 90 ms with the vast majority of kinetic energy converted into internal energy.

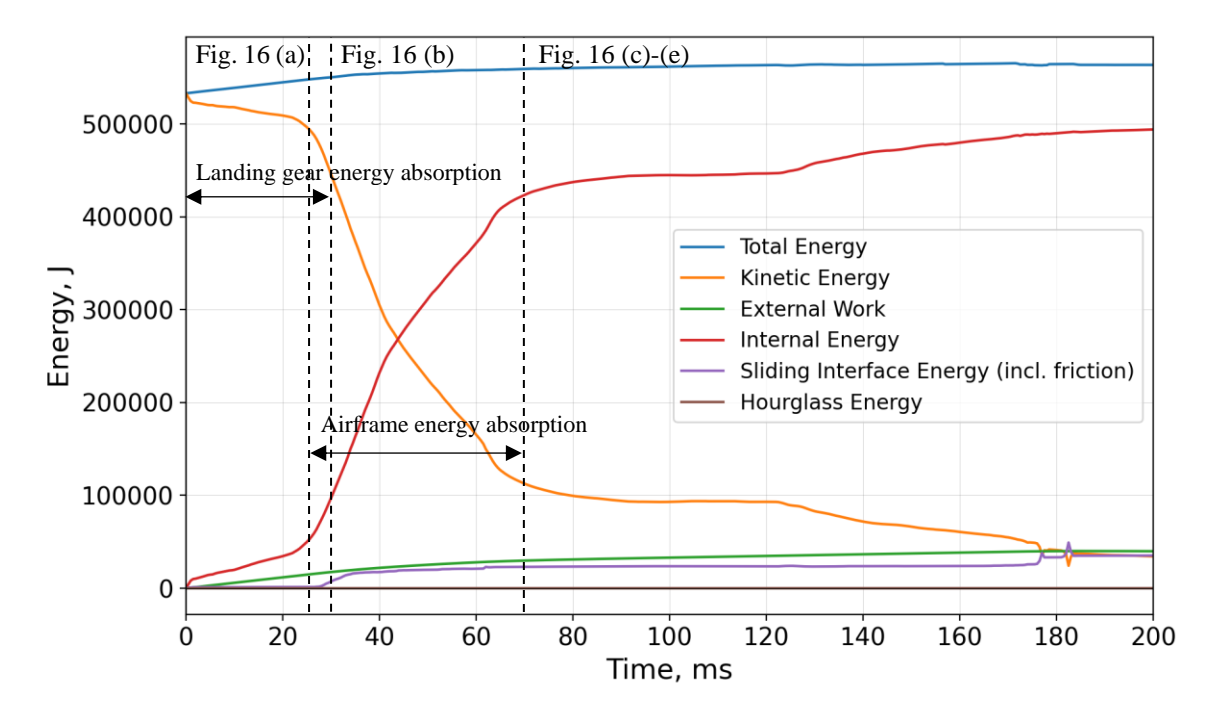


Fig. 17 Vertical impact with $v_z = 17.3$ m/s: Global energies.

Battery module accelerations in Fig. 18 show high-frequency oscillations with peak values that partly significantly exceed the specified limit of 200 g. This is especially the case for modules installed inside or between the front and rear battery pod attachments, while the modules installed outside or forward of the front attachment respectively behind the rear attachments featured comparably less oscillation peak values. As those exceedances of the acceleration limit are transient-dynamic the duration may come into play in terms of 'acceleration-duration' as a more suitable criterion, as discussed in Chapter IV-C.

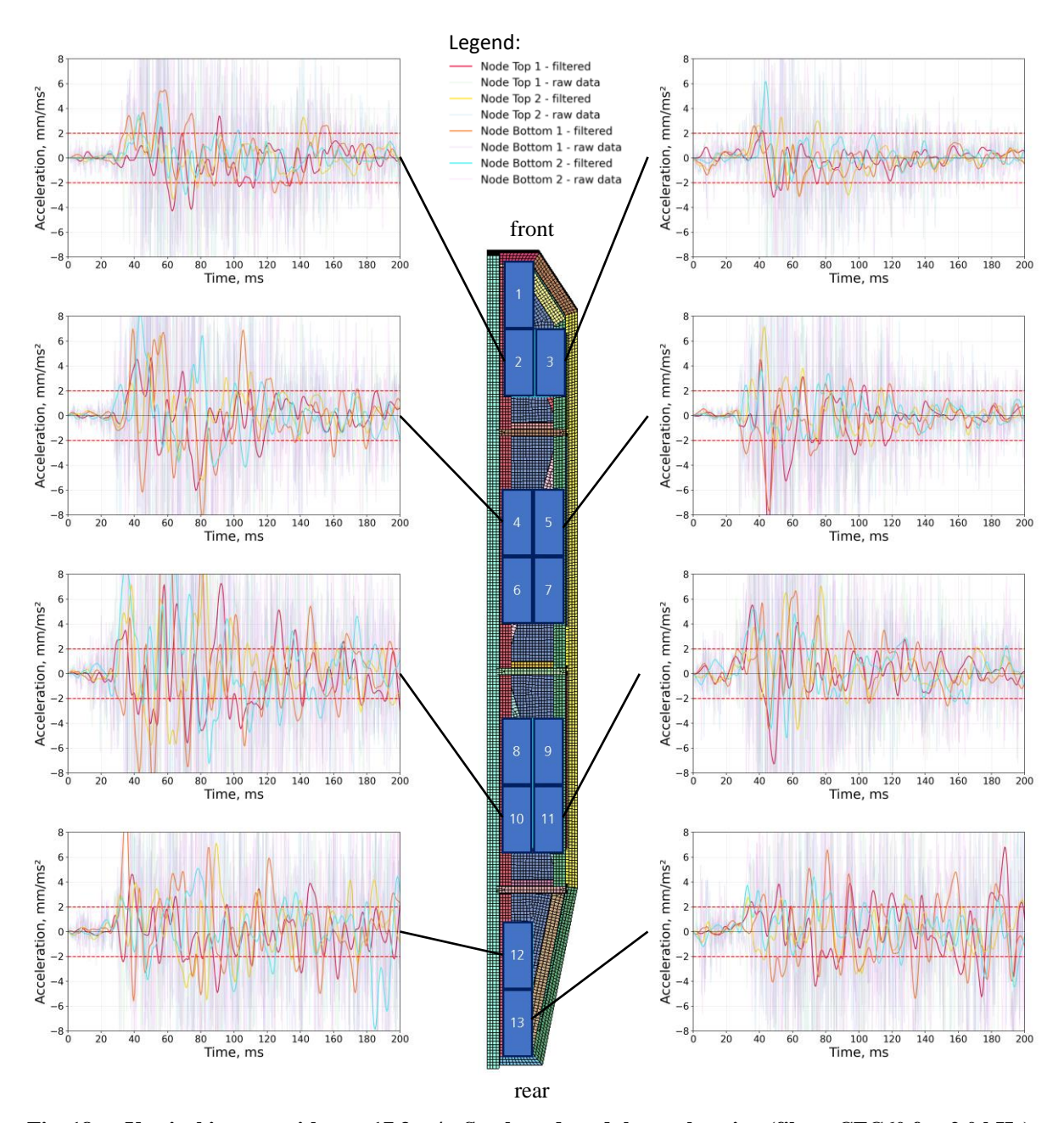


Fig. 18 Vertical impact with $v_z = 17.3$ m/s: Starboard module acceleration (filter: CFC60 $f_s = 2.0$ kHz).

Compared to the to the previous load cases, Fig. 19 shows that energy is permanently absorbed by some battery modules, especially those close to the front and rear attachment points. As the battery pod structure experiences large deformations in these areas, this can be seen as an indication for potential increase of risk for a thermal runaway when battery modules are positioned close to regions of extensive structural deformations.

At modules 12 and 13, which are positioned at the inside and rear of the pod, the first and highest peaks in internal energy can be observed at approx. 30 ms. Module 10, which is positioned forward of the rear landing gear, shows peak values which are significantly smaller and close to values seen in module 11, which is located outside. Contact interaction of the landing gear bending beam and battery pod with more distinct loads at the inner side and in rear modules is reflective of the observations in the load case with $v_z = 7.9$ m/s. The peaks in internal energy for modules 2 to 5, which are located at the forward landing gear bending beam, can be seen at approx. 45 ms. These peaks are grouped by their position along the pod length, not their positioning inside or outside the pod. This evaluation of internal energies indicates an increase in thermal runaway risk at positions closer to the rear.

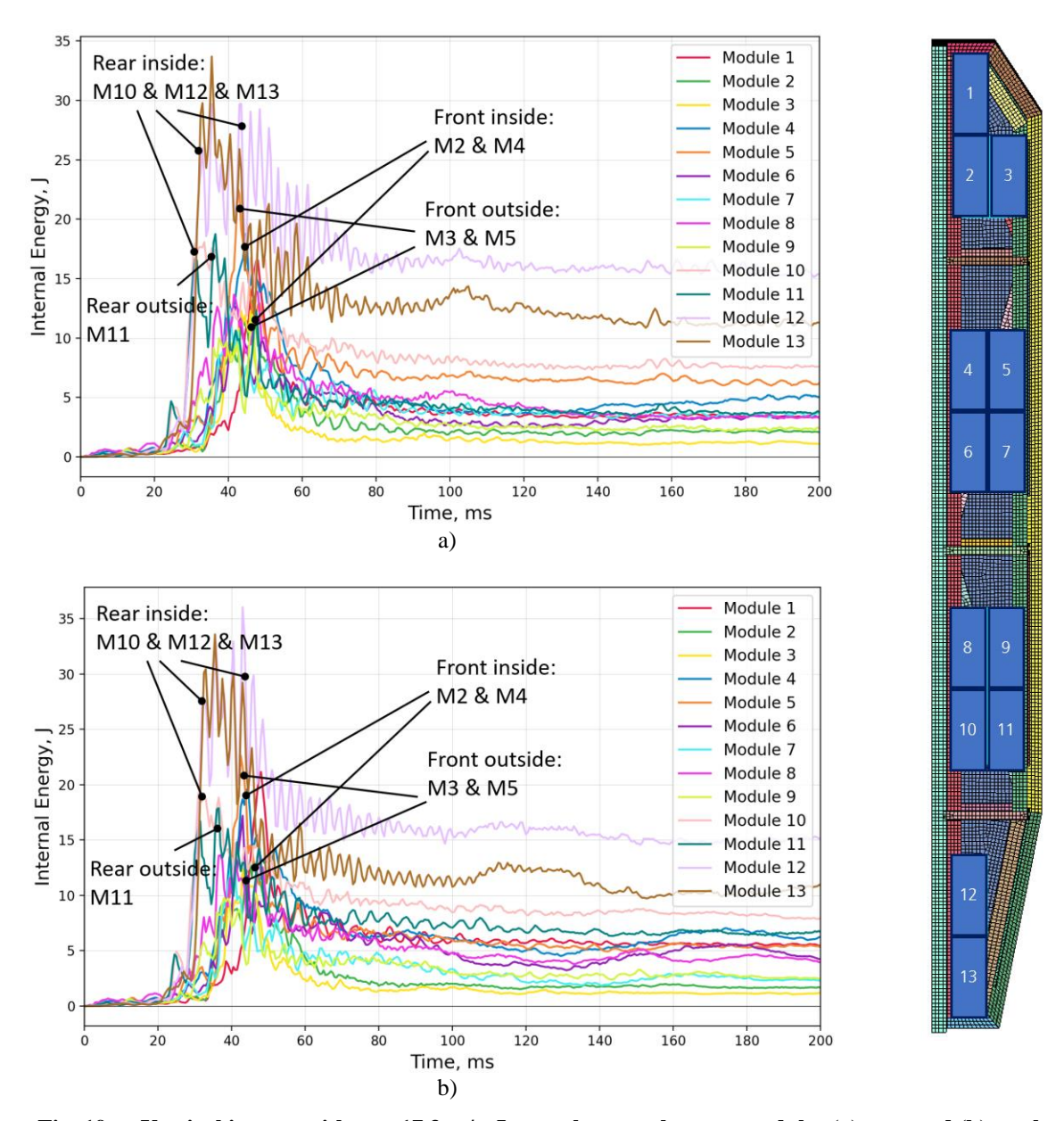


Fig. 19 Vertical impact with $v_z = 17.3$ m/s: Internal energy battery modules (a) port and (b) starboard.

Similar to the load case with $v_z = 7.9$ m/s, slightly different trends can be derived from acceleration and internal energy evaluation. Identifying the most suitable pass/fail criterion remains an active area of research, though internal energy may provide a more holistic view of the battery pod's response.

Summarized, the reference load case for the "survivable emergency landing" category shows generally favorable crash kinematics. The landing gear pushes the external battery pods upwards and out of the airframe crash zone while the such triggered separation of airframe and battery pod generally enables independent crushing and respectively load attenuation. The battery acceleration peak loads partly exceed the acceleration limits which needs to be further evaluated in consideration of the peak durations, due to the high-frequency oscillations. As a major effect, the battery pod still shows a tendency to develop a bending hinge at its center position, as a result of the contact interaction with the landing gear, although structural integrity is maintained. Those effects need to be considered in case of a more densely pod packaging. Although the evacuation path assessment is not a criterion for the "survivable emergency landing" category, the simulation results nevertheless indicate clear challenges for the evacuation path respectively accessibility of the cabin for rescue workers due to the battery pods located alongside the H/C airframe.

4. Robustness

To further extend the simulation matrix, a comprehensive robustness analysis was performed, investigating the effects of horizontal velocity, off-axis boundary conditions, rocky, uneven or soft terrain and water impact. A selection of robustness load cases is shown in Fig. 20, featuring the impact velocity of the described "survivable emergency landing conditions" ($v_z = 17.3 \text{ m/s}$).

For small roll angle load cases (see Fig. 20 (a)-(b)), an unrolling of the airframe increases the loads at the opposite side of the impacting side. For large roll angles (around 30°, see Fig. 20 (c)-(d)), interaction between the airframe and battery pod at the impacting side also increases. The landing gear bending beams fail due to axial compression loads, which significantly changed the crash kinematics. As a result, battery modules at the impacting side experience higher crash loads. In addition, large roll angles dampen the slap down effect because of more severe structural deformation and consequently less unrolling. Still, in both cases, favorable crash kinematics is observed with the battery pod at the impacting side being pushed upwards by the landing gear and hence preventing critical crushing of the battery pod and keeping it outside the crash zone.

<u>Pitch angle</u> variation also result in observable slap down effects due to airframe unrolling after first impact. The landing gear interacts differently with the impact surface compared to other load cases. Due to the unrolling, contact of the rear and front parts of the landing gear can be identified in different time steps. Slightly higher battery pod loads at the front modules can be observed. For pitch angles with "survivable emergency landing" impact velocity (vz = 17.3 m/s), a clear bending hinge develops in the battery pod structure. This can be explained by the more severe impact velocity that leads to distinct ground contact of the battery pod rear end introducing large moments that end up in the formation of this bending hinge. This is an interesting aspect as for this load case the bending hinge is not caused by landing gear interactions but instead by direct ground contact at the rear end. Hence, risk of formation of bending hinges for the battery pods is given by several reasons respectively different loading conditions, and hence the formation of a bending hinge for this long battery pod design generally needs to be considered.

Summarized, the simulations of various off-axis impact conditions reveal a general robust crash behavior and favorable crash kinematics.

<u>Horizontal velocities</u>, as additional velocity component, increase the absorbed internal energy due to additional deformation of the battery pod structure. This indicates higher structural loads due to the battery pod mass inertia featuring additional horizontal velocity components. Still, very similar effects are obtained compared to the baseline load case with purely vertical impact – at least for a sliding friction between H/C and ground specified with a friction coefficient of $\mu=0.19$. Higher friction coefficients representing other terrain conditions might lead to more severe effects.

The <u>combination of vertical and horizontal impact velocities with off-axis angles</u> (see Fig. 20 (e)-(f)) generally shows results that are similar to the load cases without combinations. In total, the crash condition does not reveal more severe damage or battery pod loading than obtained in other load cases. Effects identified there occur in a combined way for this load case, while these effects did not sum up to more severe or critical failure. The results generally show favorable crash kinematics.

A <u>one-sided sloped impact surface</u> (see Fig. 20 (g)-(h)) does not lead to an unrolling of the airframe. Again, and even for this severe condition, the landing gear pushes the battery pod upwards out of the crash zone and prevents critical crash interactions between airframe and battery pod.

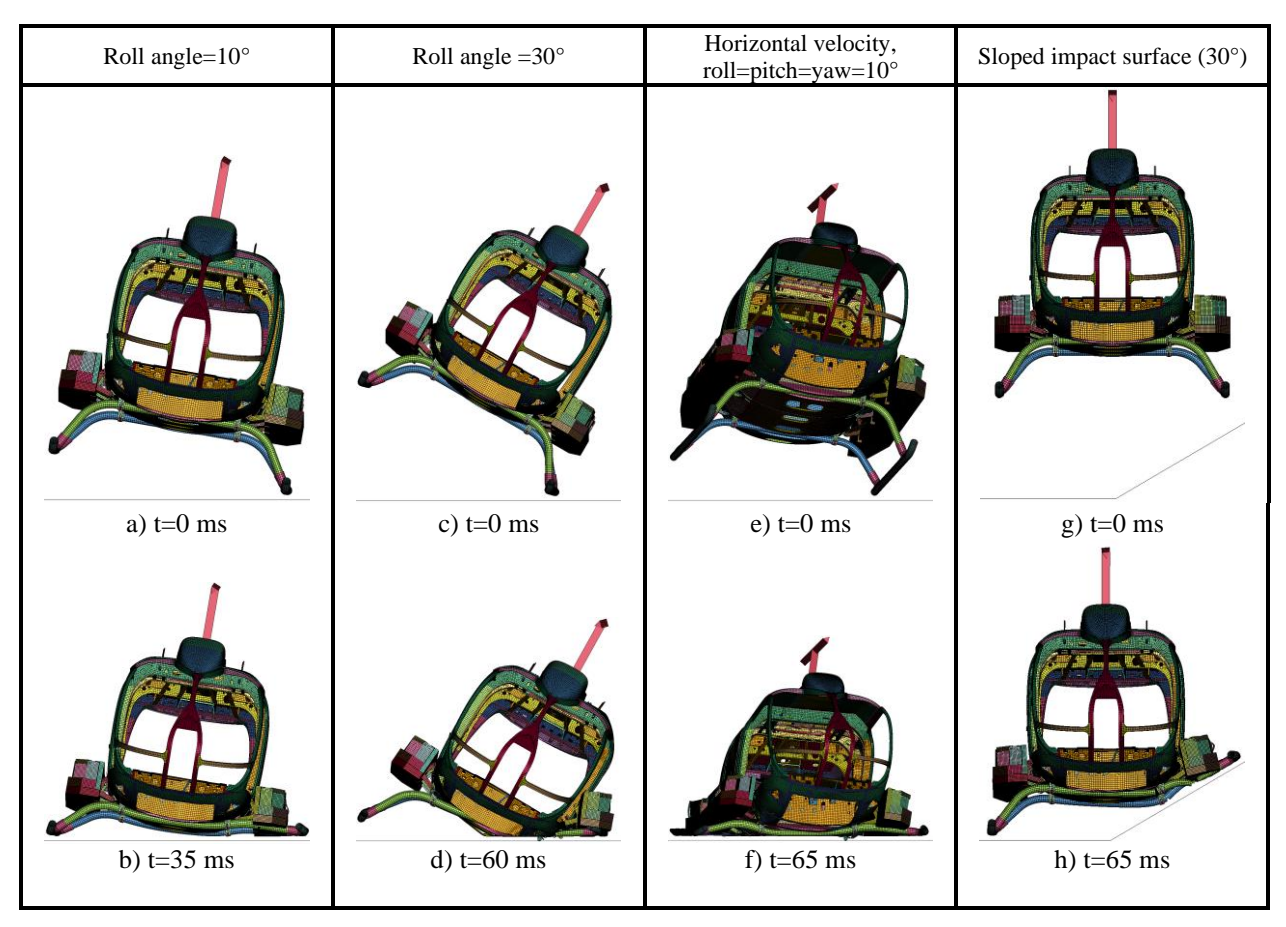


Fig. 20 Selection of robustness load cases with v_z=17.3 m/s.

All robustness load cases show favorable crash behavior, underlining the significance of the detachment mechanism, decoupling the kinematics and load of the airframe and the battery pods. In addition, the important effect of the landing gear pushing the battery pod out of the crush zone between H/C airframe and ground decrease the interaction between pod and airframe. The combination of the landing gear pushing the battery out of the crush zone and the detachment mechanism enabling structural separation can be seen as a key design parameter for obtaining the identified favorable crash robustness.

VI. Conclusion

A. Battery Pod Technology Brick Evaluation

Multiple technology bricks were conceived in Chapter IV-A and implemented in the investigated integration design. This included volumetric crash absorbers, a heat resistant containment, a vent pipe concept, special integration guidelines for surrounding airframe structures and a separation and intrusion attachment mechanism. All these technology bricks were implemented and evaluated.

The integrated **volumetric absorbers** have shown to provide full-surface load transfer of crash loads, significantly reducing the accelerations experienced by the battery modules during a crash. Additionally, they provided protection against penetration by external bodies as their increasing compression, hence densification, also acts as protective shielding. This protection also reduced the consequences of the battery pod interaction with the landing gear, which introduced loads locally into the battery pod structure. Lastly, their superior crash characteristics when encountering soft impact surfaces and water were shown.

Due to the use of surrogate battery models, the **containment** aspect was not investigated in more detail by the performed numerical simulations. This aspect can only be investigated in more detail after integrating surrogate battery models with proper thermal runaway modelling methods, including thermal and electrochemical aspects.

The **vent pipe** has not been designed in detail in the models investigated in this report. Still, assumptions regarding the its design were reinforced with the results shown here. A positioning along the top of the battery modules proved

crucial in preventing crushing and potential blockages. The identified crash kinematic effects of the battery pod during different crash load cases confirmed the necessity of flexible vent pipes.

The **battery pod structure** was purposely designed to provide mass retention for the battery modules to prevent a catastrophic disintegration of the pod even under severe load cases. Global and local crash loads acting on the pod structure led to significant structural deformations. In this sense, structural integrity of the battery pod is a key feature in preventing battery module overloading, hence structural materials should be selected that provide sufficient ductility. The investigated load cases also clearly showed that the survivable volume of the airframe was never endangered from the selected battery pod design.

The **assembly** of battery modules in the battery pod (battery packaging), with gaps at strategic locations, assisted in reducing the loads experienced by the battery modules due to different pod deformation depending on the load case.

Interaction with surrounding structure, here between the H/C airframe and the battery pod, was largely limited through the separation mechanism. This mechanism has shown to be crucial in preserving the crash kinematics of the landing gear, especially for robustness load cases with roll angles or sloped impact surfaces. However, no intrusion of the battery pod into the H/C underfloor structure was observed for all load cases, because of the favorable interaction of the landing gear and the battery pod.

B. Method

Multiple FE models were developed to evaluate the crashworthiness of the battery integration design. The developed models are considered to be sufficiently accurate for conceptual design phases considering crashworthiness.

Prior to the conduction of the full-scale simulation campaign of the entire H/C airframe with installed battery pods, several preliminary studies using simplified and downscaled models were conducted, showing that an increase in structural complexity of the integration structure typically also increases acceleration oscillation and is strongly depended on the selected local point of measurement. This increased the difficulty of evaluating the risk of a thermal runaway during crash based on measured accelerations.

All acceleration results were filtered with SAE J211-1 [17] CFC60 filter. This increased the readability of the acceleration results, but not enough to compensate for the described effects. This leads to the consideration of whether 'acceleration versus pulse duration' may be a more suitable criterion for thermal runaway evaluation at airframe integration level. However, this evaluation criteria requires more detailed battery test data.

Therefore, the internal energy of each battery module was additionally evaluated as an alternative measure for the assessment of thermal runaway. This method enables the observer to study the effect of crash conditions on selected battery modules based on their change in internal energy – as a measure of structural loading respectively structural deformation. While the residual internal energy represents material damage, failure, and plastic deformation, the elastic deformation can also be analyzed based on short term internal energy changes. This method is particularly useful in evaluating the risk of thermal runaway across multiple battery modules, identifying the biggest source of thermal runaway risk for more detailed evaluations. However, an absolute risk assessment based on this criterion requires battery test data and differentiation of load types like local indentation and global deformation of the battery module. Additionally, following this approach one has to keep in mind potential modelling simplifications of the battery modules that can affect the measure of internal energy.

A battery surrogate model has been used in all studies instead of fully modelled battery modules with cells. This surrogate model only represents inertia, mass and stiffness of a real battery module. The internal battery module structure is not captured, mainly due to the lack of battery data at this early design stage, and hence structural deformation of the surrogate model is not validated. These limitations in battery surrogate modelling and in the definition of proper thermal runaway criteria is subject of current research work at DLR.

In this paper, the integration has been evaluated with generic full-scale H/C airframe models. The airframe model used has been partially validated with regard to this specific application. Load cases were derived from the CS-29.562 Reserve Energy Absorption Drop Test [10], CS-29.562 Emergency Landing Dynamic Conditions [10] and CS-29.952 Fuel System Crash Resistance Test [10]. The simulation matrix was concluded with simulations investigating the robustness of the battery integration. The developed models and load cases have shown to be sufficiently accurate and extensive for this conceptual design study as important effects and trends are clearly visible.

C. General Trends

The investigated load cases effectively showed the behavior of the designed battery pod with surrounding structures like the landing gear and airframe during crash. Interaction between the landing gear and battery pod increases with increased impact velocity, particularly between the landing gear bending beam and battery pod bottom absorbers. The following effects can be observed across all investigated load cases:

Battery pods are pushed out of the crash zone. Deformation of the landing gear pushed the battery pods upwards before airframe-ground contact, preventing the pod from being crushed or intruded into the underfloor structure. This favorable interaction confirms the concept's feasibility and robustness even under severe crash conditions.

Traditional airframe subfloor crushing occurred in all simulations, with battery pods mainly contacting the landing gear or ground at higher impact velocities. No adverse effects on subfloor crushing were observed.

Battery packaging requires consideration of pod crash kinematics, as the elongated pod mainly impacted the landing gear bending beams, with minimal ground contact at impact velocities up to $v_z = 7.9$ m/s. The impact results in hinge-like deformation at the pod center and local pod structure deformations at bending beam contact positions. For higher velocities ($v_z = 17.3$ m/s) ground contact can be observed while hinge-development is initiated but not fully developed. In robustness load cases with non-zero pitch angles, hinge development is initiated by ground contact of the pod rear. These effects underline the need to consider hard points of the airframe and landing gear, as well as deformation and kinematic behavior of the pod structure for the battery packaging concept as battery modules should not be positioned in these critical zones.

The **separation mechanism as a key design principle** enabled independent crash kinematic of the battery pod and H/C airframe, enabling the battery pod to get pushed out of the crash zone.

Considering the overall H/C model, **battery pod absorbers** only marginally contributed to overall energy absorption, with most energy being absorbed by the airframe and landing gear. This is reasonable, as the battery absorbers are solely related to the battery pod mass of 354 kg, not the entire airframe mass. About 60 % of external pod's impact energy (53 kJ at $v_z = 17.3$ m/s) was absorbed by the pod absorbers, while the rest was dissipated by the pod structure or detachment from the airframe. Due to interaction with the landing gear, the absorber experienced non-uniform loading, concentrating energy absorption at interaction points. The partial energy absorption by pod structures must be considered in later design stages, as they must maintain integrity during crash.

Besides energy absorption, the pod absorbers protected and stabilized the structure by distributing landing gear loads into the pod. Volumetric absorbers proved effective not only for water impact, but also for non-uniform loading, as typical absorber compaction provides shielding.

Simulations showed that only bottom and inside absorbers are relevant in mitigating crash loads, bottom absorbers reduced vertical loads and inside absorbers reduced airframe interaction, especially during roll angles. Other absorbers may be removed in future design iterations.

Investigating battery module loads with regards to locations of structural deformation showed that modules installed between front and rear pod attachment experienced high-frequency oscillations with peak values partly significantly exceeding specified limits. In contrast, modules installed forward of the front or behind the rear attachments oscillated less. Internal energies evaluation confirmed these trends, correlating higher energies with areas experiencing higher deformations. This indicates a potentially increased risk of thermal runaway when modules are positioned close to regions of extensive structural deformations.

Since the battery pod **surrounding structure** is located near the modules, their interaction may not fully be shielded by absorbers and may transfer crash-induced deformations directly into the modules. The pod structure must therefore be designed to avoid excessive deformation or failure near modules, and especially must prevent risk of battery module intrusion by broken structural parts. This principle, well established in CRFS design guidelines, must be applied for battery integration as well.

The maintenance of a safe **evacuation path** remains a key challenge, as pods positioned alongside the H/C airframe may hinder accessibility of the cabin for rescue workers. Besides structural integrity, key pod features include crashworthy containment and venting systems to ensure evacuation paths remain free of post-crash hazards.

Acknowledgments

Parts of the research leading to these results were accomplished in the framework of the 6th Aeronautical Research Program of the German Federal Ministry of Economic Affairs and Climate Action (BMWK) under grant 20M2114C, as part of the LuFo-VI-2 project NEUTRON. The authors wish to thank Michael Geiss, Sascha Schneider, Marc Nothen, Stefan Böhnel, Martin Blacha and Johannes Röthinger from Airbus Helicopters for great collaboration in this research project.

References

- [1] Ohnishi, M., Yoshimura, T., and Hirano, M., "A crash test of a BK117 helicopter," Proceedings of the JSASS/JSME 27th Structures Conference, pp.300-303 (in Japanese), 1985.
- [2] Robertson, S.H., Johnson, D.S., Hall, D.S., and Rimson, I.J., "A Study of Helicopter Crash-Resistant Fuel Systems," U.S. Department of Transportation Final Report DOT/FAA/AR-01/76, 2002.

- [3] Bennett, C.V. and Schroers, R.J., "Impact Tests of Flexible Nonmetallic Aircraft Fuel Tanks Installed in Two Categories of Simulated Wing Structures," CAA Technical Development Report No. 291, 1957.
- [4] Robertson, S. Harry, and Turnbow, J.W., "Aircraft Fuel Tank Design Criteria," USAAVLABS Technical Report AvSER 65-17, 1966.
- [5] Johnson, N.B., Rogers J. H., and Cook R. L., "Aircraft Fuel Systems Design Study," USAAVLABS Technical Report 67-33, 1967.
- [6] Robertson and H, S., "Development of a Crash-Resistant Flammable Fluids System for the UH-1A Helicopter," USAAVLABS Technical Report 68-82, 1969.
- [7] Cook Richard L. and Donald E. Goebel, "Evaluation of the UH-1D/H Helicopter Crashworthy Fuel System in a Crash Environment," USAAMRDL Technical Report 71-47, 1971.
- [8] Coltman, J.W., "Rotorcraft Crashworthy Airframe and Fuel System Technology Development Program," FAA Final Report DOT/FAA/CT-91/7, 1994.
- [9] European Union Aviation Safety Agency, "Certification Specifications, Acceptable Means of Compliance and Guidance Material for Small Rotorcraft (CS-27) (Amendment 10)," EASA, 2023.
- [10] European Union Aviation Safety Agency, "Certification Specifications, Acceptable Means of Compliance and Guidance Material for Large Rotorcraft (CS-29) Amendment 11," EASA, 2023.
- [11] European Union Aviation Safety Agency, "SC E-19 Electric / Hybrid Propulsion System," EASA, 7th 2021.
- [12] European Union Aviation Safety Agency, "Special Condition for small-category VTOL-capable aircraft Issue 2 (SC-VTOL-02)," 2024.
- [13] European Union Aviation Safety Agency, "MOC SC-VTOL (Issue 2)," EASA, 12th 2021.
- [14] Lewis, E., "Ditching, Emergency Flotation and Limited Overwater Operations," Rotorcraft and VTOL Symposium 2020 (Virtual Event), November 12th 2020.
- [15] "Aircraft Crash Survival Design Guide, Volume V Aircraft Postcrash Survival," USAVSCOM Final Report TR-89-D-22E, 1989.
- [16] Wegener, E., "Crashworthy Battery Integration for a Medium-Lift Hybrid-Electric Helicopter," *Proceedings of the 50th European Rotorcraft Forum (Structures and Materials)*, Marseille, France, 2024.
- [17] Chou, C.C., Lin, Y.S., and Lim, G.G., "Instrumentation for Impact Test Part 1 Electronic Instrumentation: SAE J211-1 (2022)," *SAE Technical Paper Series*, SAE Technical Paper Series, International Congress & Exposition, MAR. 01, 1993, SAE International Commonwealth Drive, Warrendale, PA, United States, 1993.